



Computational-Experimental Study of Plasma Processing of Carbides at High Temperatures

Arturo Bronson and Vinod Kumar
Department of Mechanical Engineering
University of Texas at El Paso

Program Manager: Richard J. Dunst
National Energy Technology Laboratory
DOE Award – FE0008400



High Temperature Research

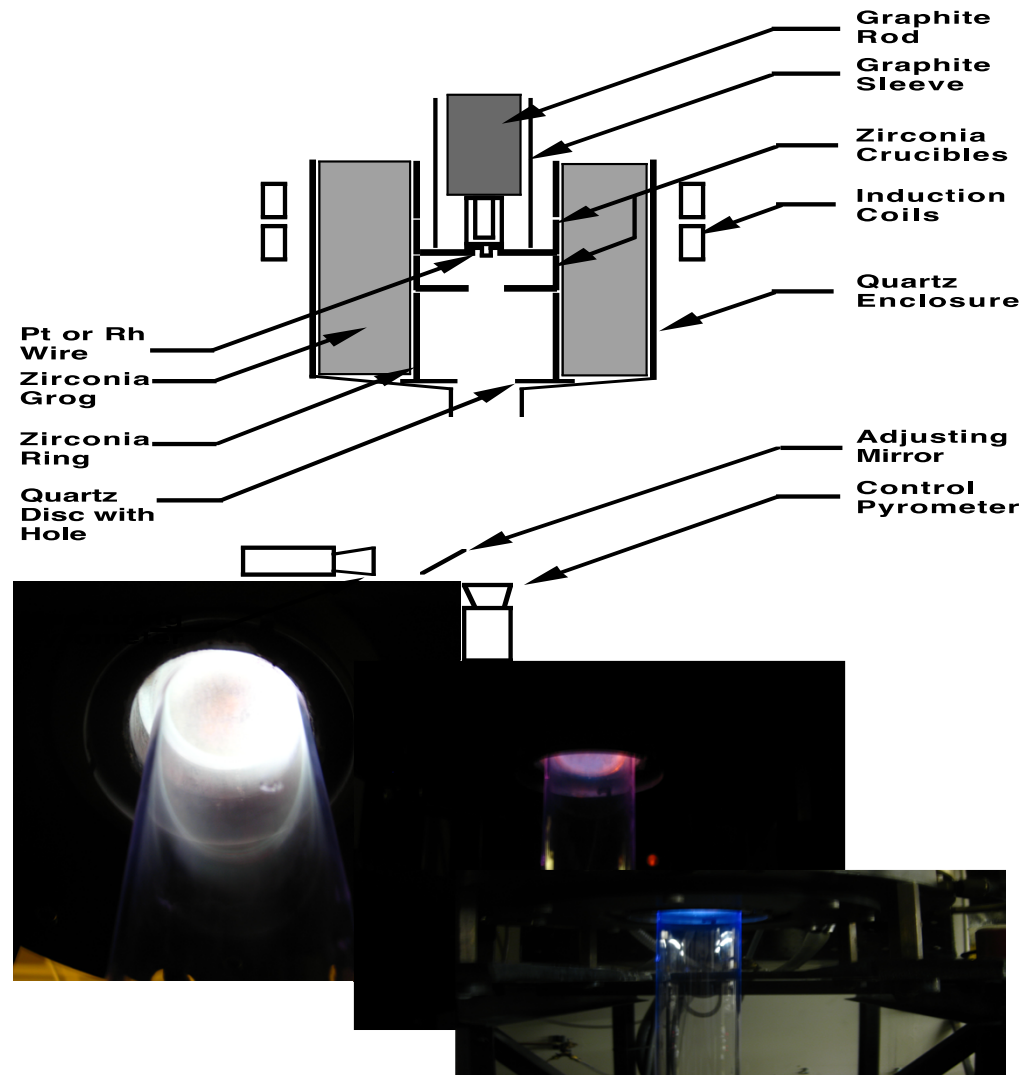
- **Graduate Students**
 - Alejandro Garcia (Computational - Masters)
 - Arturo Medina (Computational - Masters)
 - Sanjay Shantha-Kumar (Experiment - Ph.D.)*
- **Senior/Graduate Student Transition**
 - Alberto Delgado
(Experimental/Computational – Dual B. S. in Mechanical Engineering with B. S. in Metallurgical & Materials Engineering)

* Aids students in high temperature research.



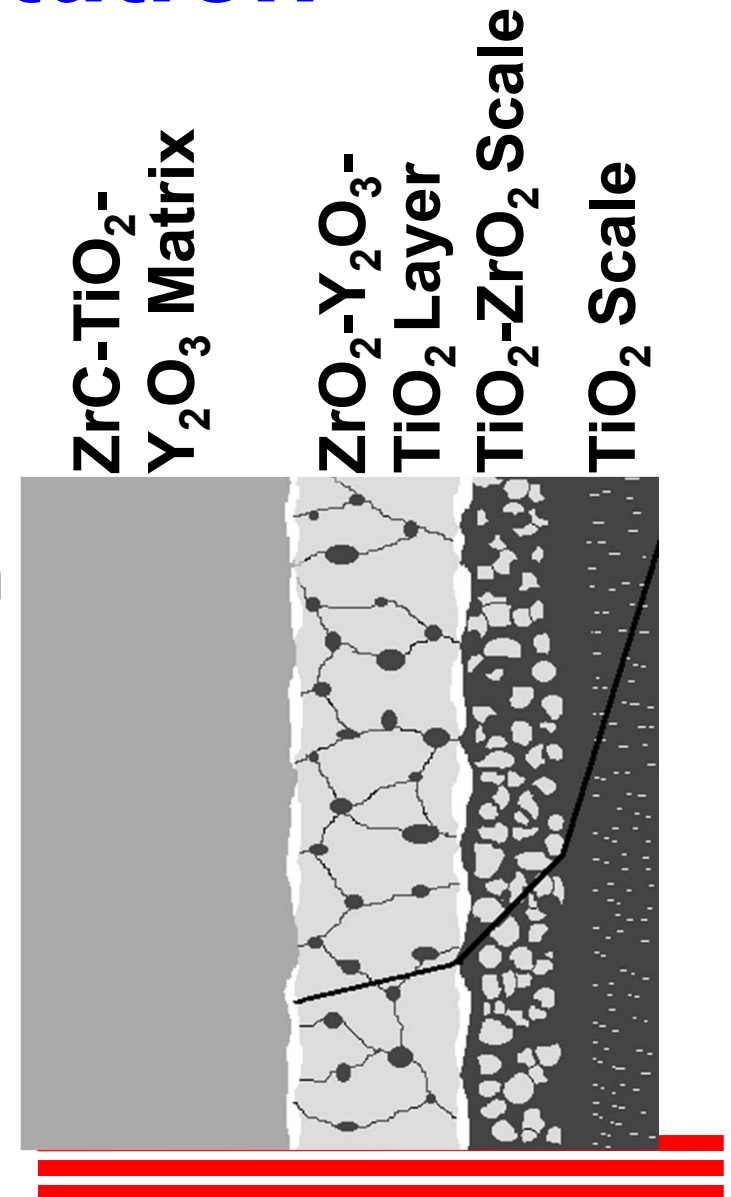
Motivation/Impact of Research

- Use electromagnetics to **control plasma surface reactions.**
- Use plasma processing to **create temperature extremes.**
- Use temperature spikes to **form metastable phases.**
- Use electromagnetics to **change diffusional flux.**



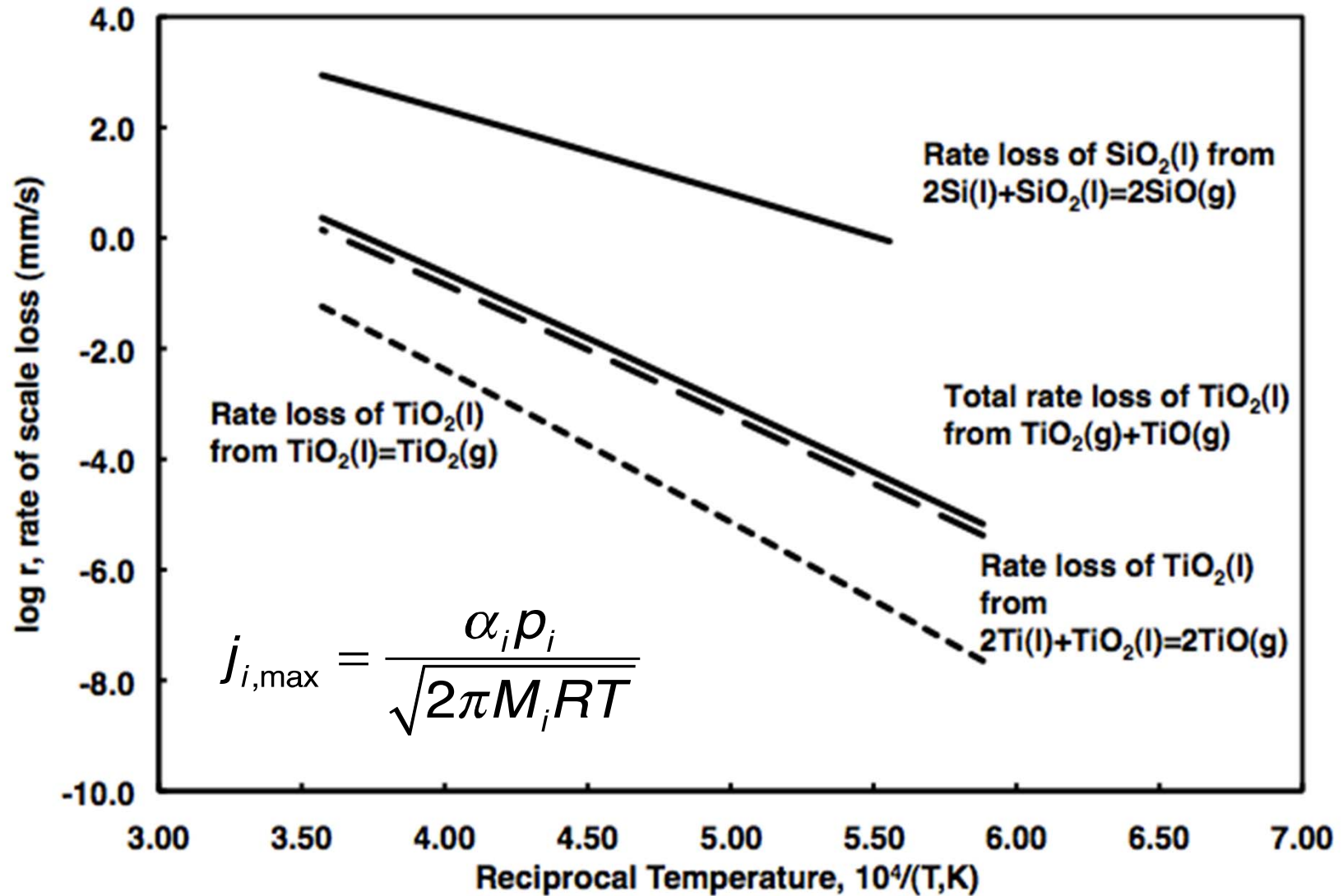
Outline of Presentation

- Introduction – Processing
 - Scale of Al_2O_3 and TiO_x
 - Packed Bed Reactivity
 - Plasma Surface Reactions
- Computational Effort – computational thermodynamics coupled with heterogeneous kinetics infused with fluid dynamics to model plasma gas reactions
- Strategic Experimentation – $\text{Ti}_3\text{AlC-TiC-Y}_2\text{O}_3$, SiC , $\text{ZrC-TiO}_2\text{-Y}_2\text{O}_3$
- Progress and Analysis



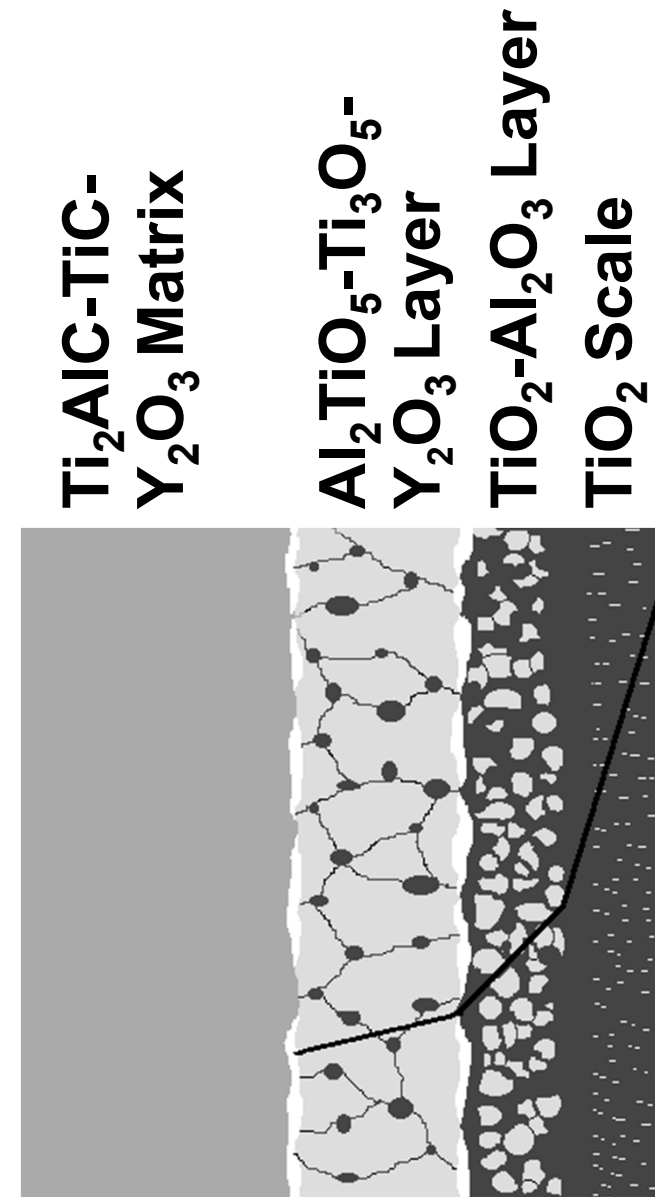


Vaporizing Flux of SiO_2 and TiO_2



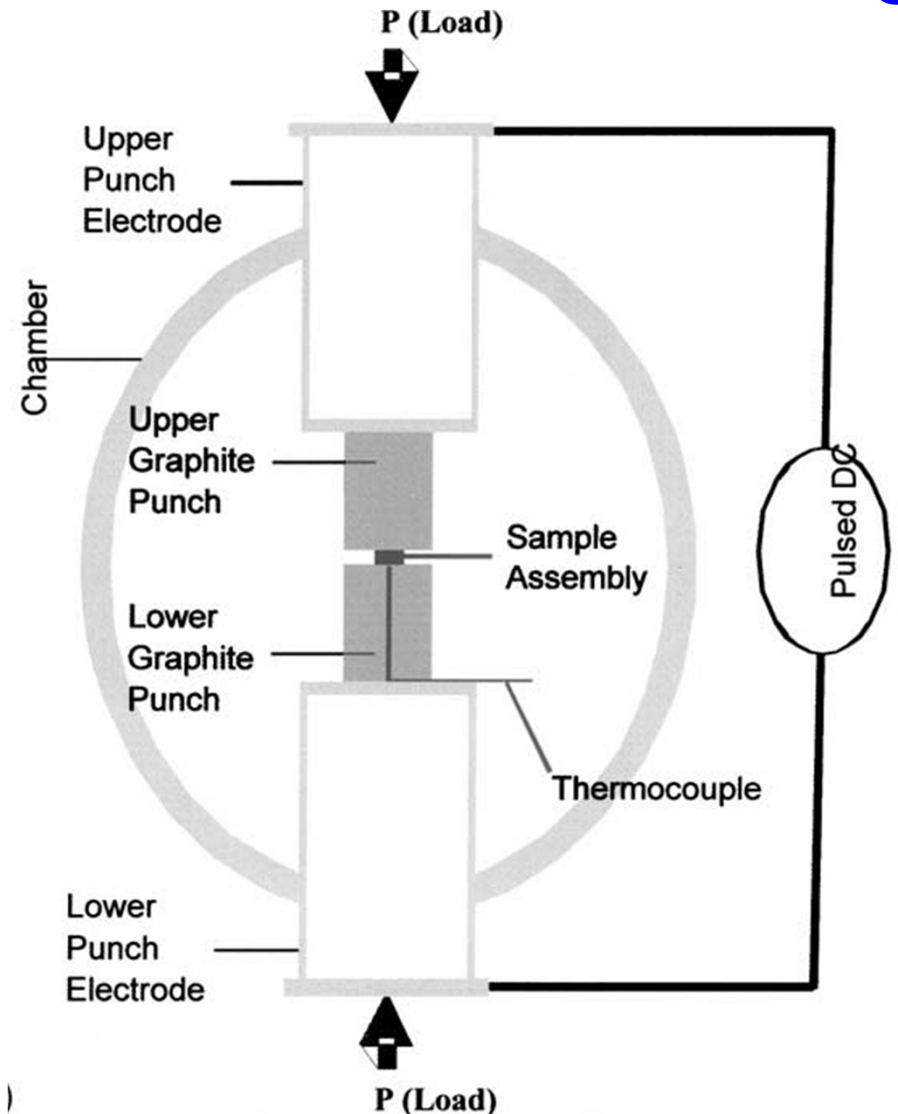
Project Objectives

- Investigate the effects of plasma surface reactions within pores of carbide packed bed;
- Investigate the effect of the potential gradients of the electromagnetic field on mass transfer;
- Investigate the effect of temperature spikes on pore surfaces.



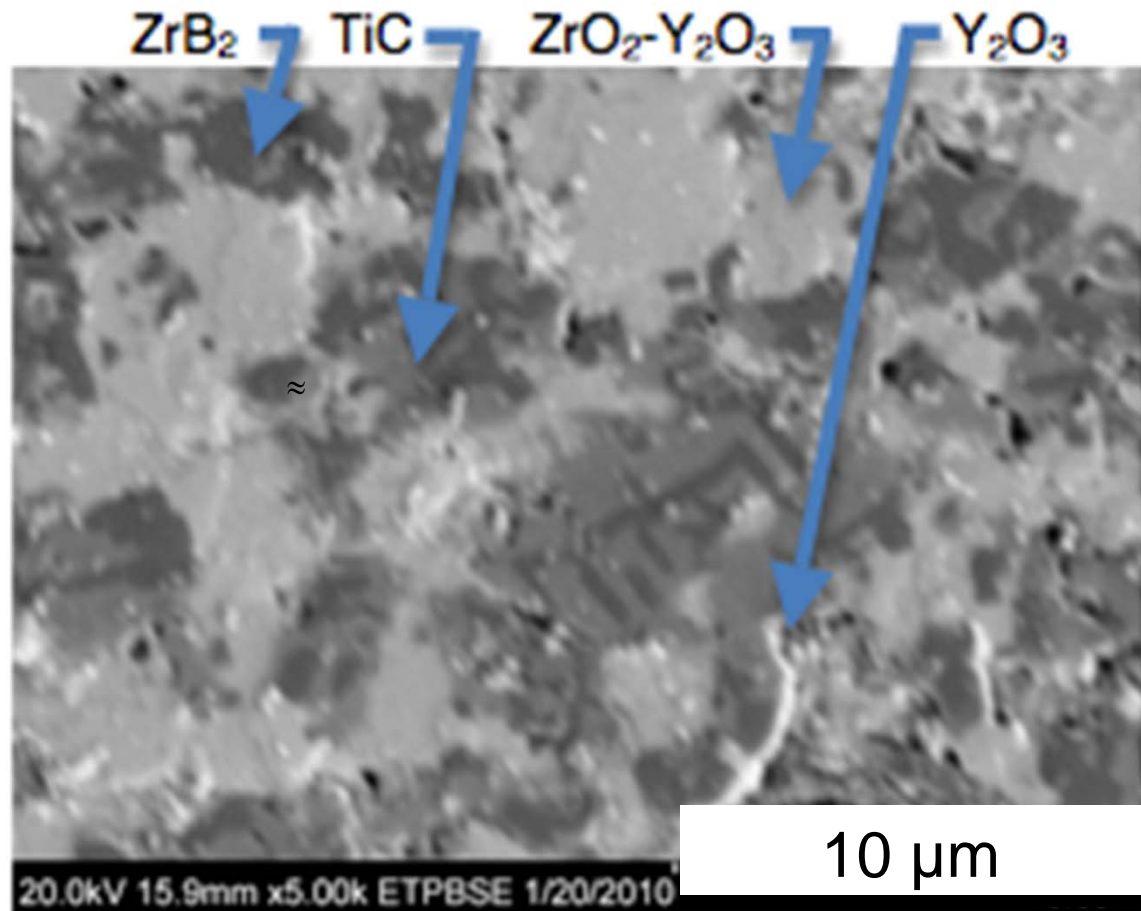
Thoughts on Spark-Plasma Sintering

- Plasma has been professed to enhance sintering but **without ionized gas evidence**.
- Current pulses passes through graphite – sample though **configuration affects the temperature extremes developed**.
- What **percentage of electromigration and thermal diffusion** contributes to sintering?



SEM image after spark-plasma sintering (SPS)* of ZrB_2 -TiC- Y_2O_3

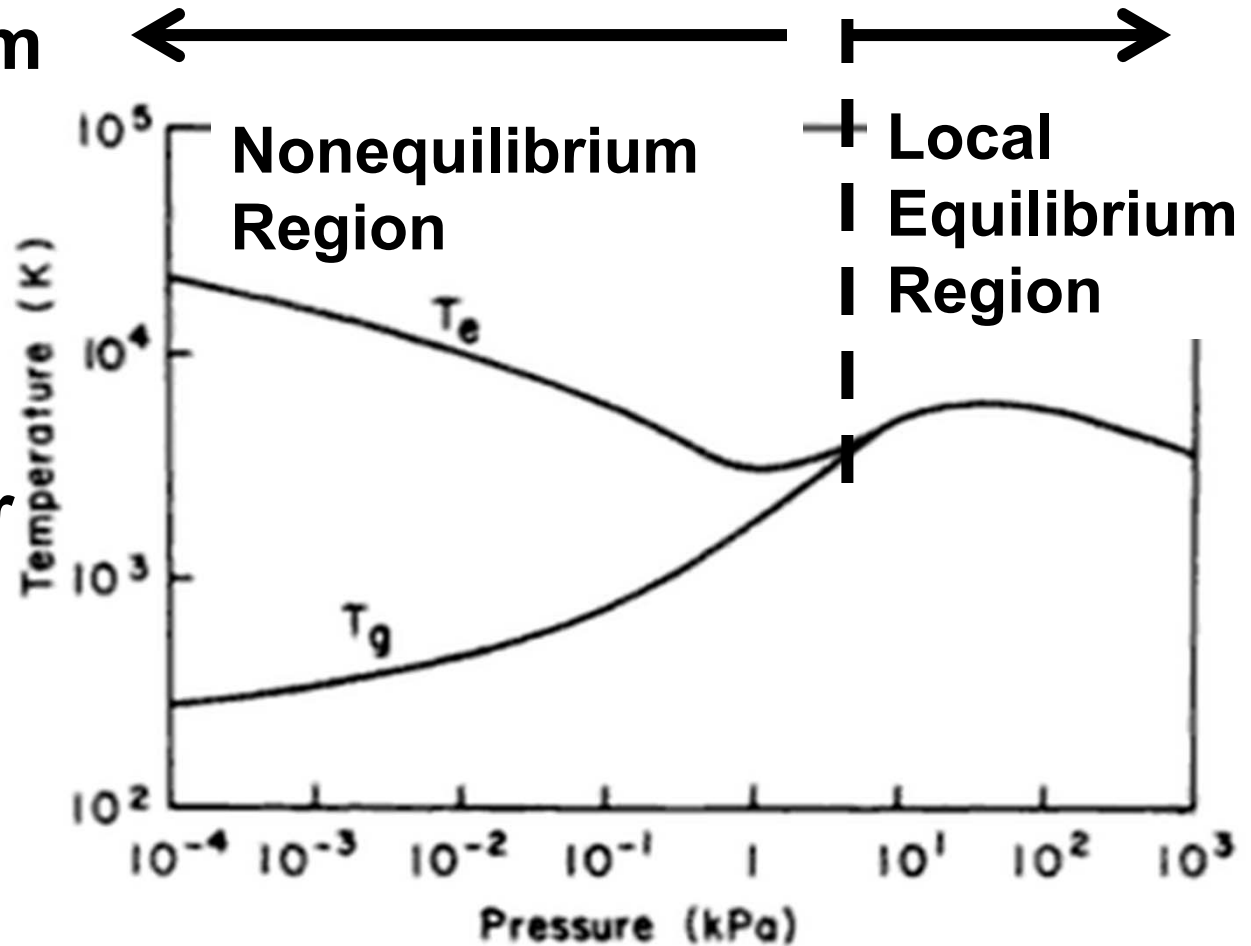
- ZrB_2 oxidizes to ZrO_2 dissolving some Y_2O_3 .
- Stringers of Y_2O_3 appear in grain boundary.
- Graphite minimized TiC oxidation though TiO formed from residual O_2 in Ar.



* SPS done at Dr. Erica Corral's Laboratory at U of Arizona

Plasma Temperatures - Pressures

- Non-equilibrium versus local equilibrium plasmas
- Plasma energy in terms of T or $(T_e - T_g)/T_e$
- Significantly lower number of studies on plasma-surface reactions.

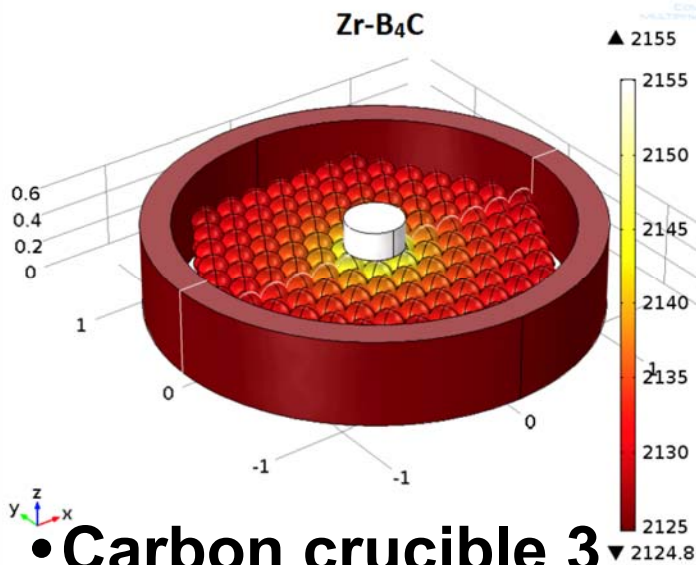


Boulous, Fauchais and Pfender--1994

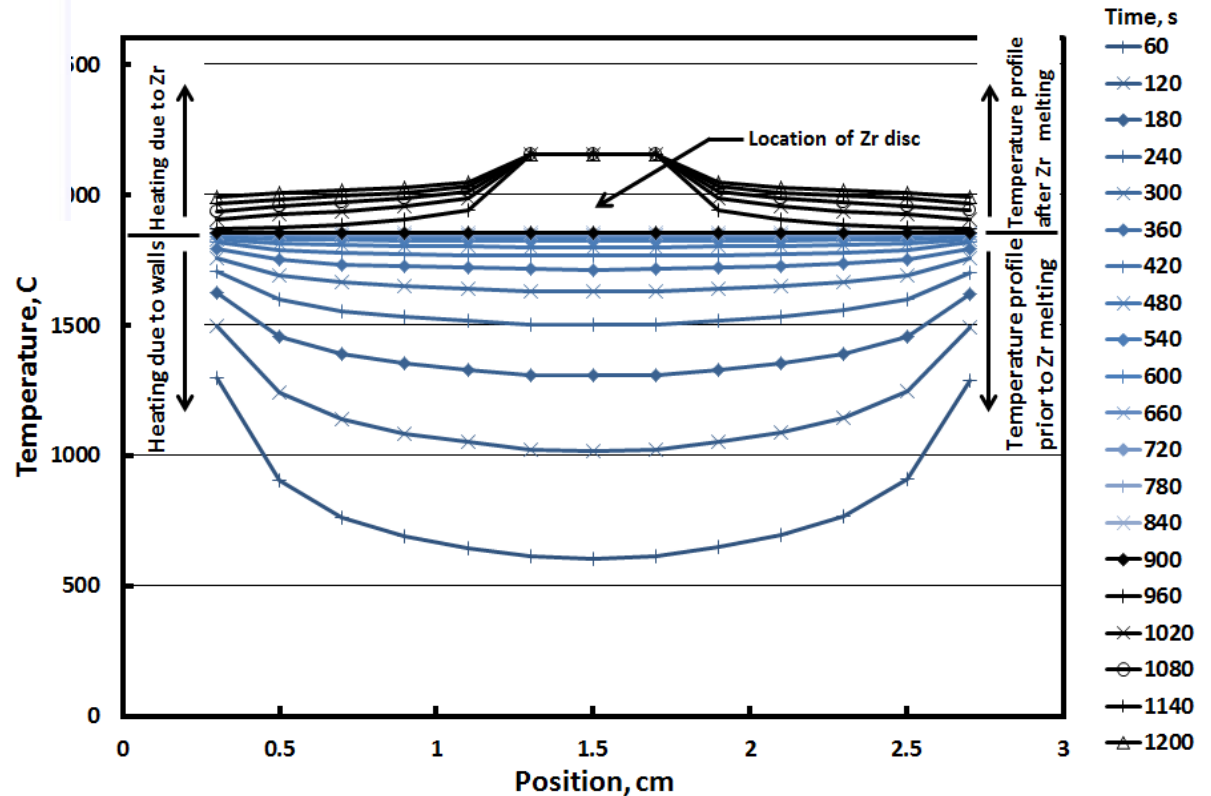


Temperature Transients from COMSOL Simulations

- B₄C packed bed (0.2 cm diameter spheres) with a Zr disc (0.4 cm diameter) placed on top of bed.
- Temperature profile of bed and Zr heating depicted.



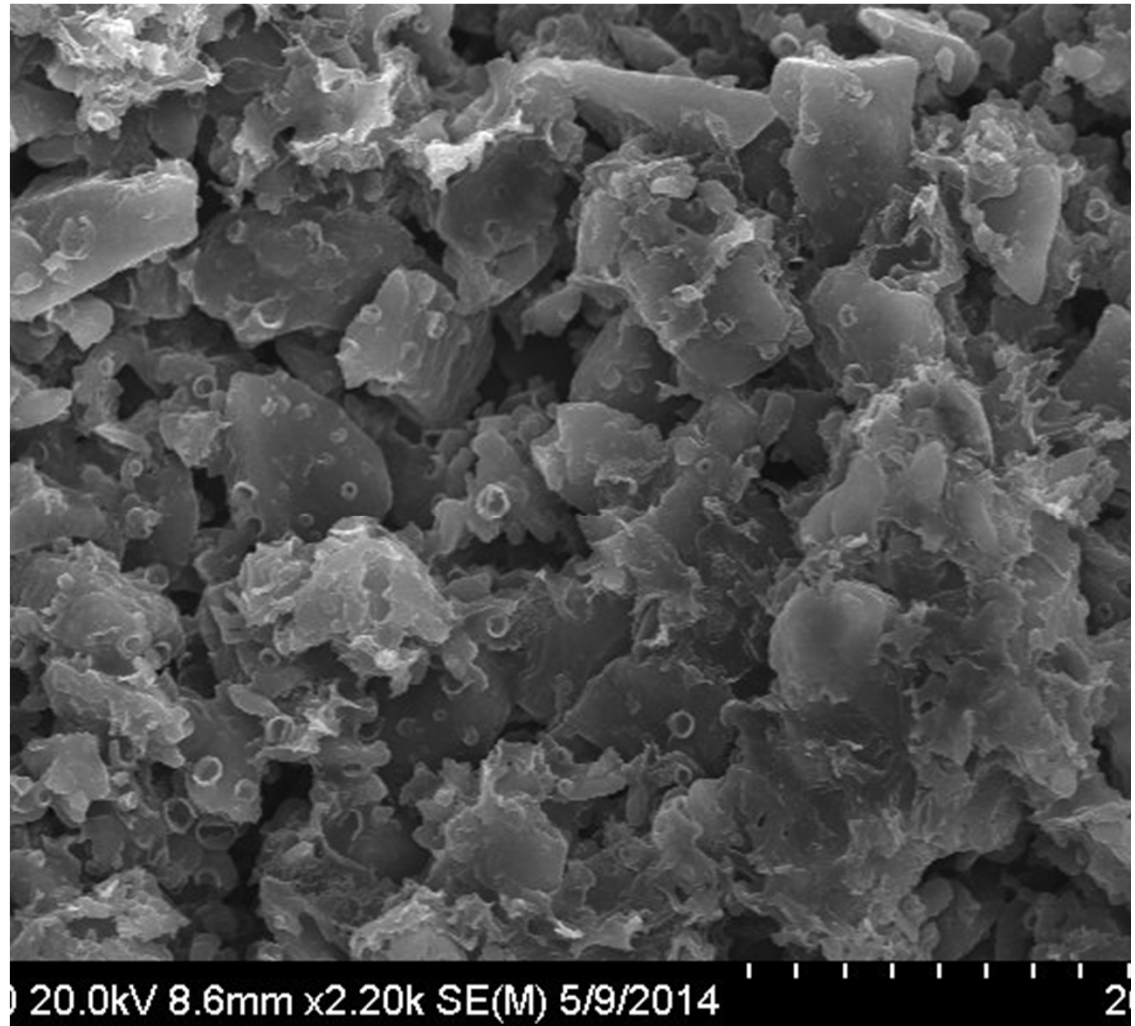
- Carbon crucible 3 cm OD-2.6 cm ID & 254 B₄C spheres.
- B₄C melts at 2450° C
- Zr melts at 1855° C
- $k_{B_4C}=4.5$, $k_{Zr}=34$ W/(mK)





B₄C Microstructure after 1700° C Heating

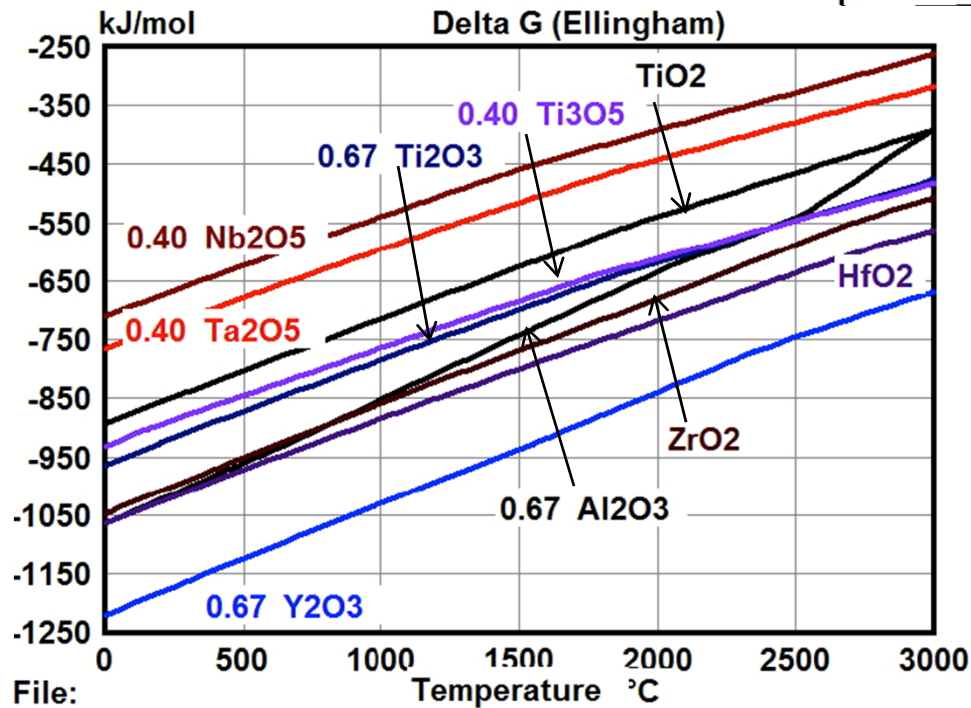
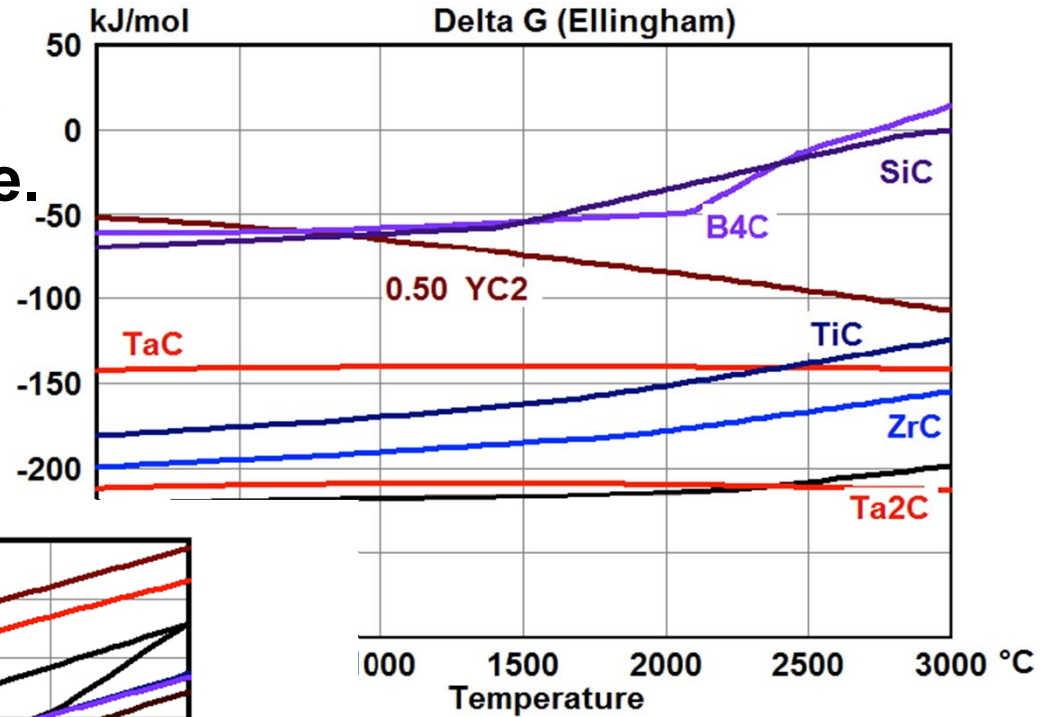
- **B₄C powder averaging 10 μm was heated to 1700° C in a graphite crucible.**
- **Afterwards, liquid Bi was used to embed particles followed by polishing.**
- **Pores vary from 1 to 10 μm.**





Stabilities-Oxides and Carbides

- For carbides, HfC, Ta₂C and ZrC are most stable.
- For oxides, Y₂O₃ and HfO₂ are most stable.
- Used Outotec HSC v. 7



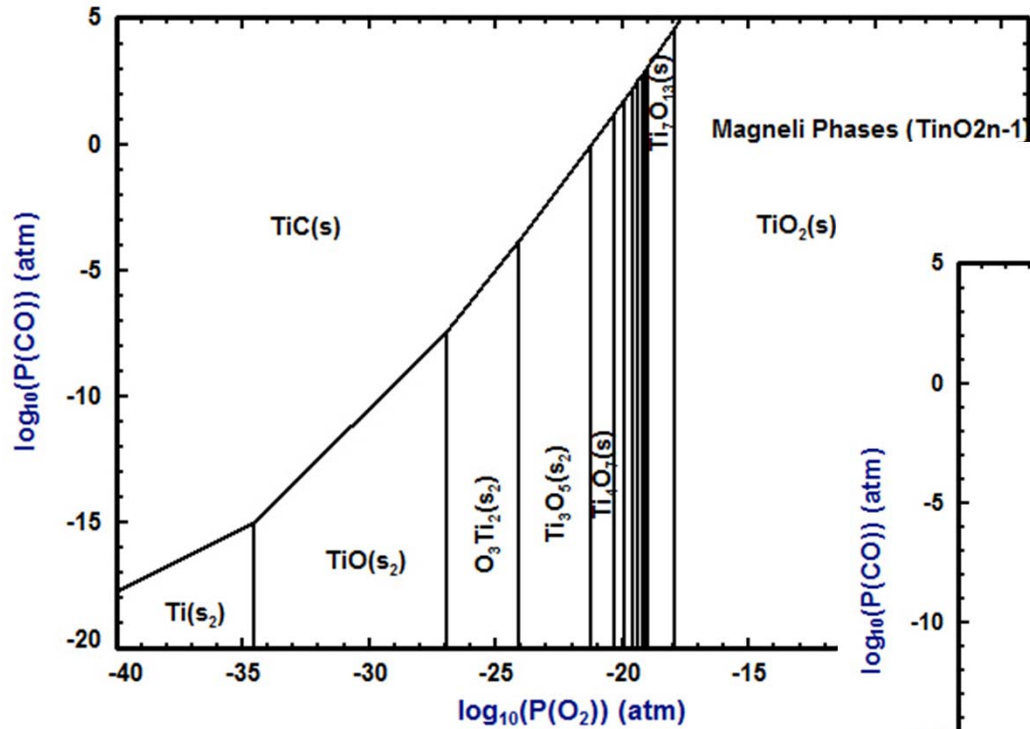
File:



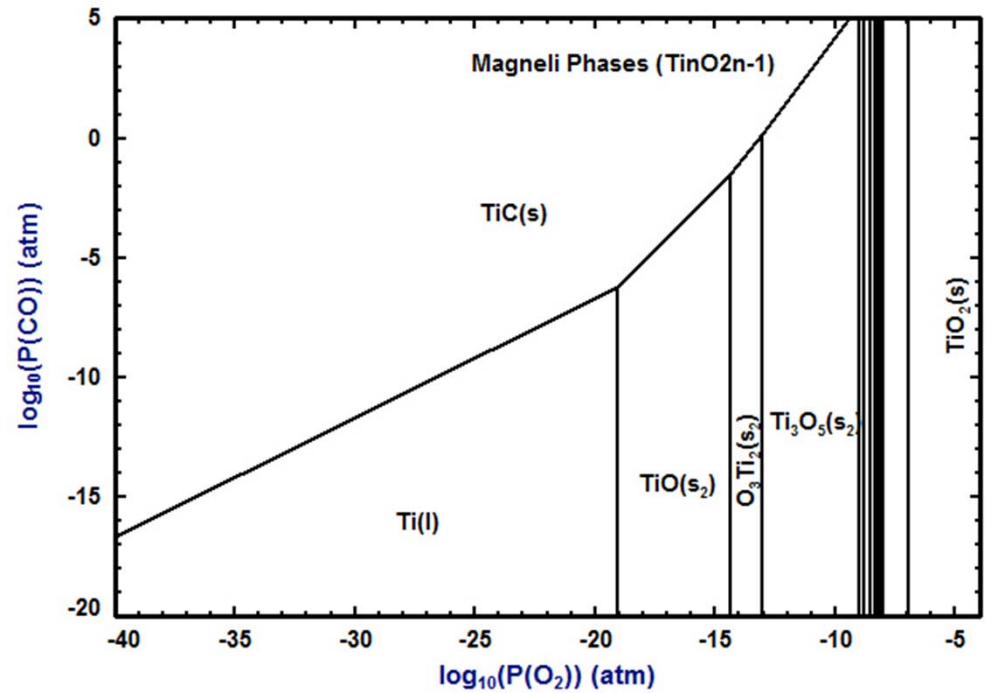


Ti-C-O Stability Diagrams at 1273 & 1973K for Expanded View of Magneli phases & p_{O_2}

Ti-C-O, 1273 K

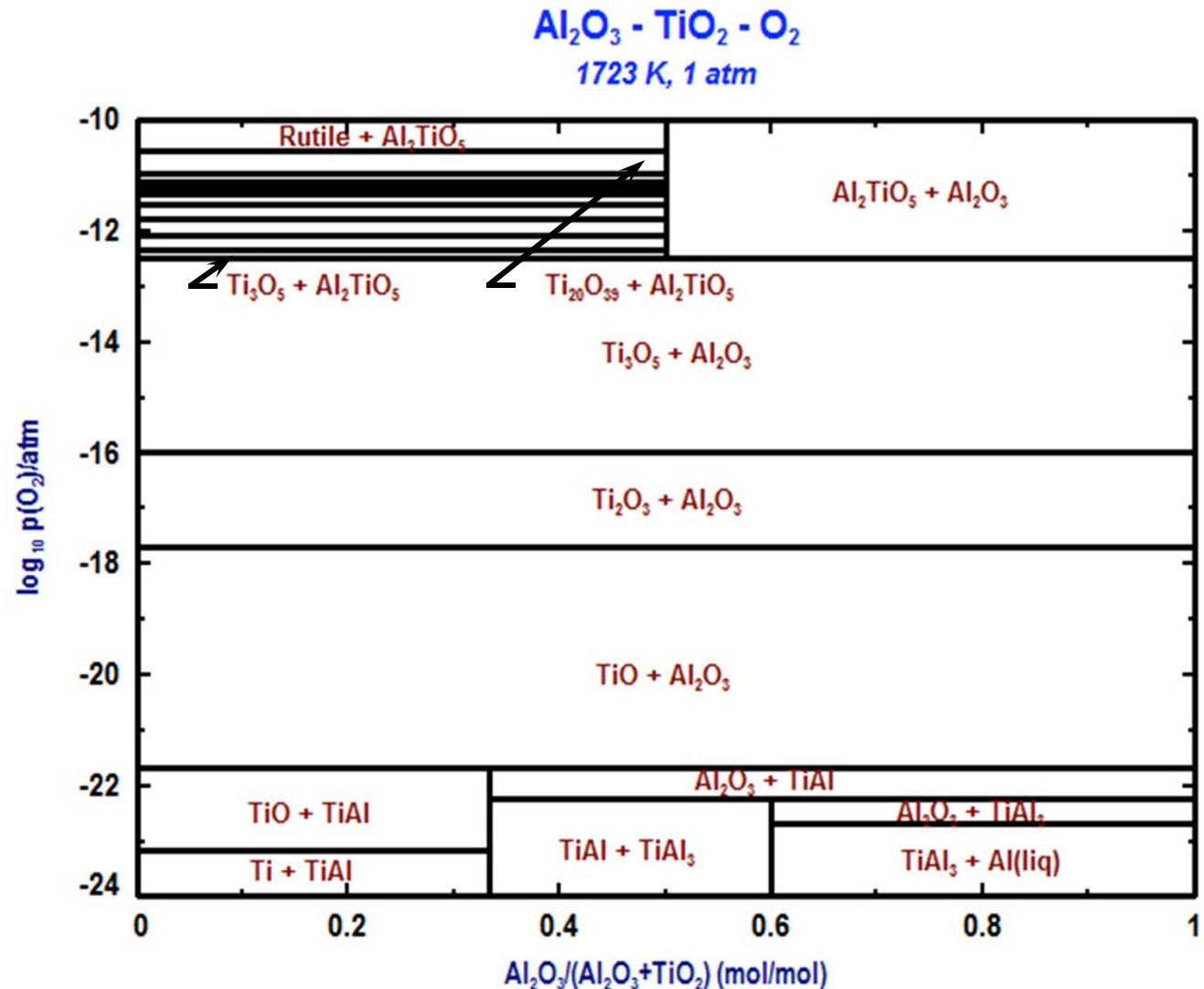


Ti-C-O, 1973 K



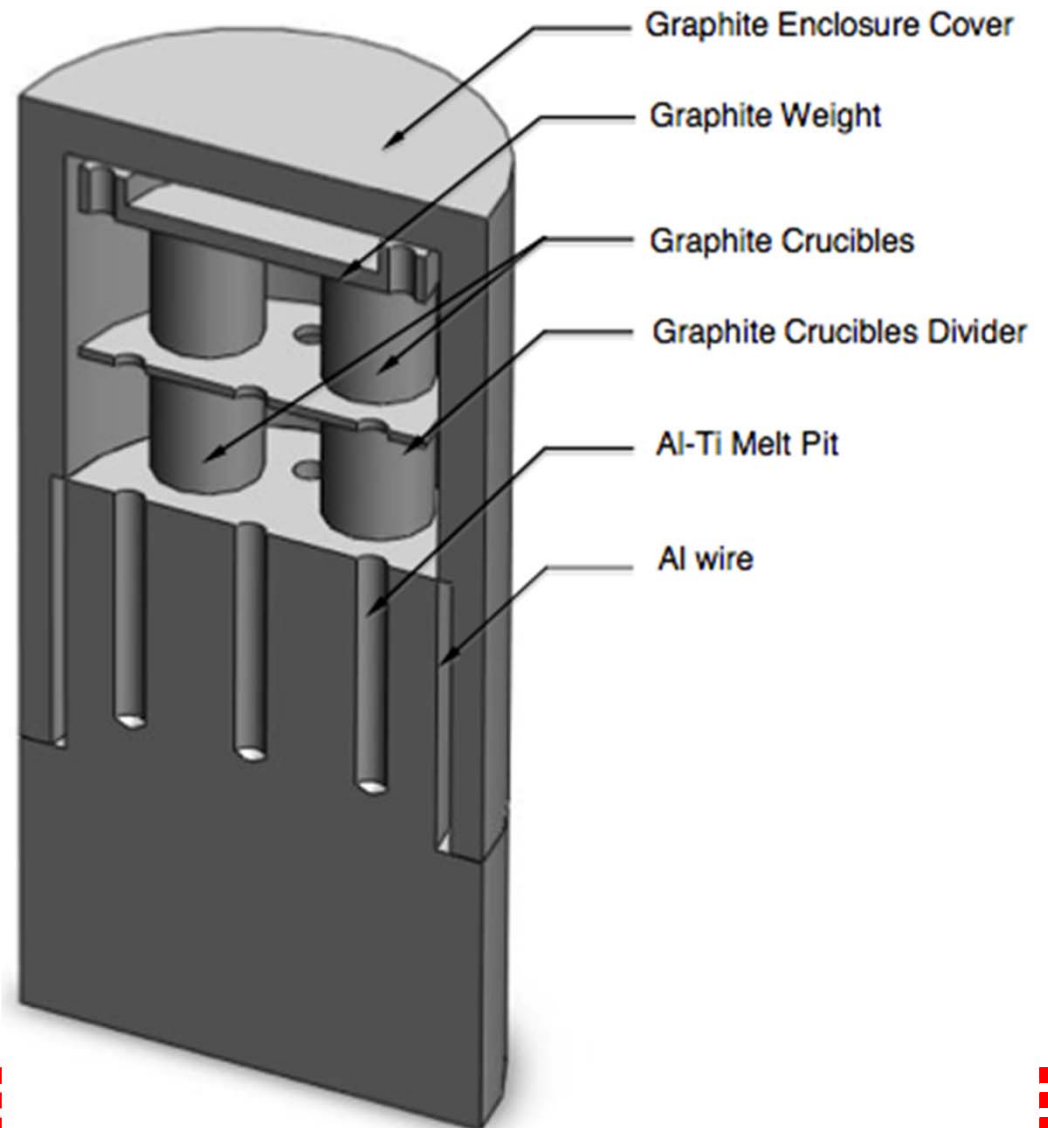
Possible Scale of Oxidized $Ti_2AlC-TiC$

- Ti oxides depend on pO_2 level within scale.
- Muan/Osborn showed limited solubility of $Al_2O_3 - Al_2O_3 \cdot TiO_2$ and $Al_2O_3 \cdot TiO_2 - TiO_2$ pseudobinaries.
- $Al_2O_3 \cdot TiO_2$ melts congruently at $1860^\circ C$ as per Muan/Osborn.

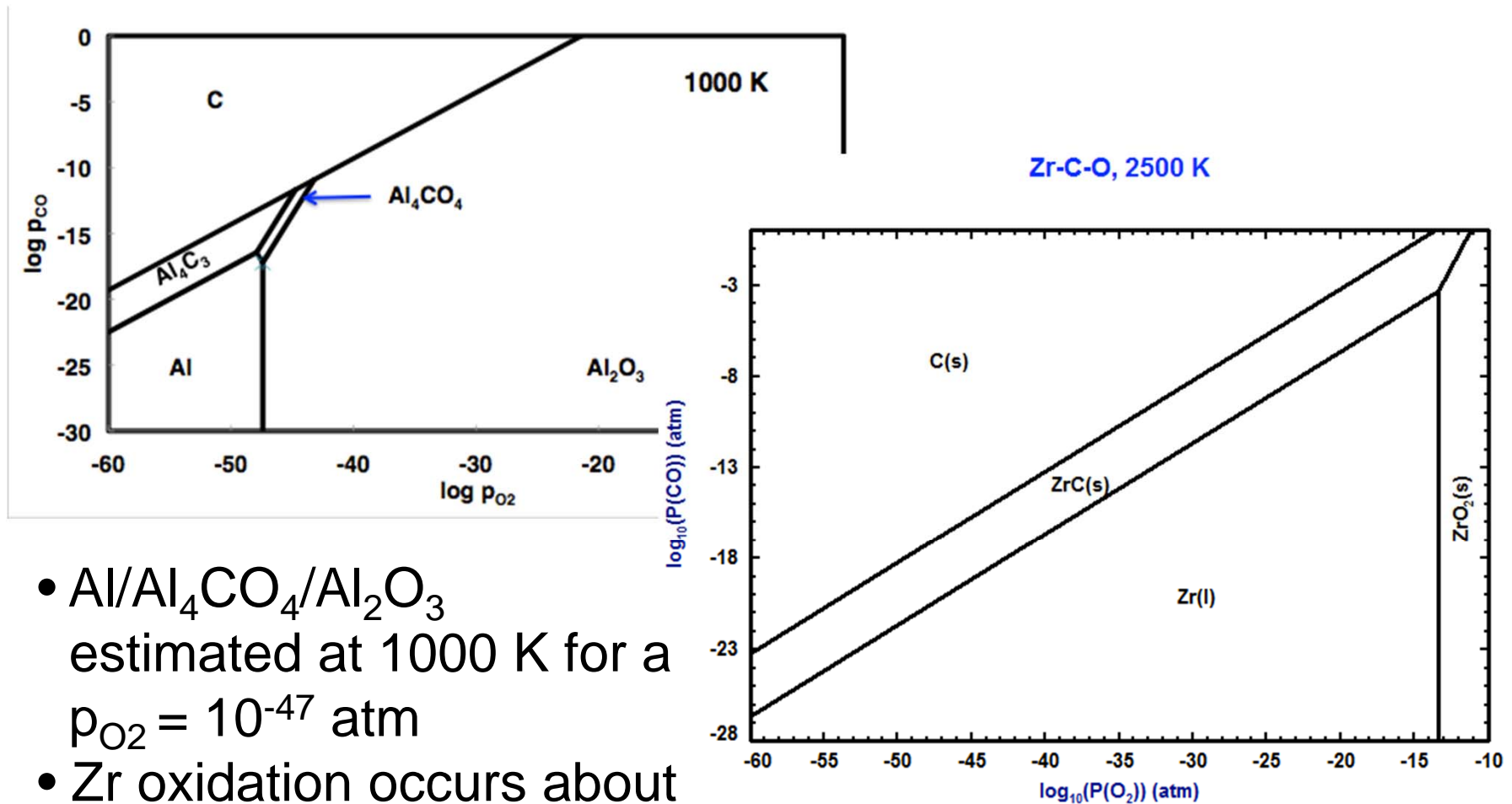


Configuration of Ti-Al-C reaction system

- Ti-Al-C charged to graphite crucibles heated to 1600-1700° C.
- Closed thermodynamic system controls oxygen potential.
- Al/Al₄CO₄/Al₂O₃ establishes p_{O₂} at 1000 K (follows concept of Komarek research group using pseudo-isopiestic technique).

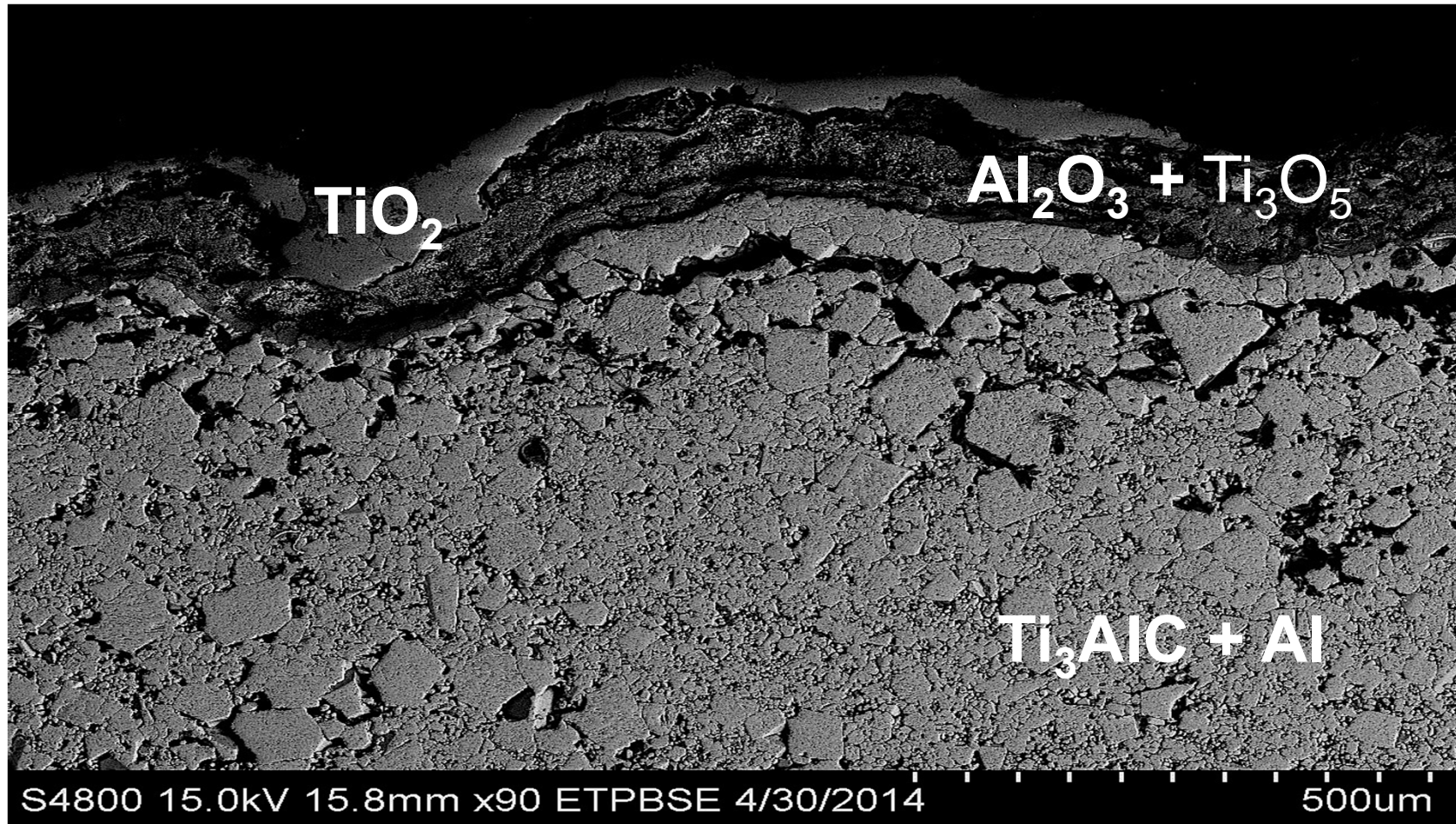


Stability of Al-C-O System at 1000 K and Zr-C-O System at 2500 K



- Al/ Al_4CO_4 / Al_2O_3 estimated at 1000 K for a $p_{O_2} = 10^{-47}$ atm
- Zr oxidation occurs about 10^{-13} atm.

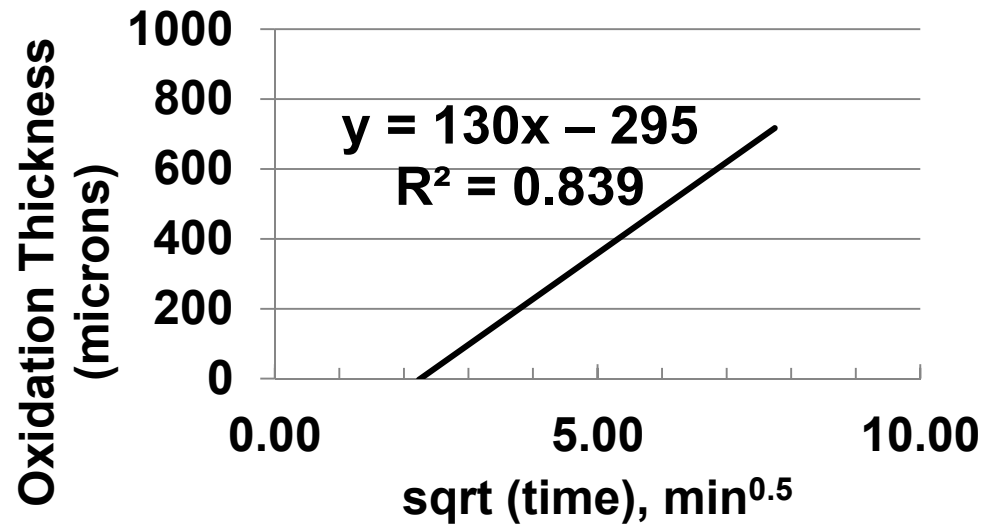
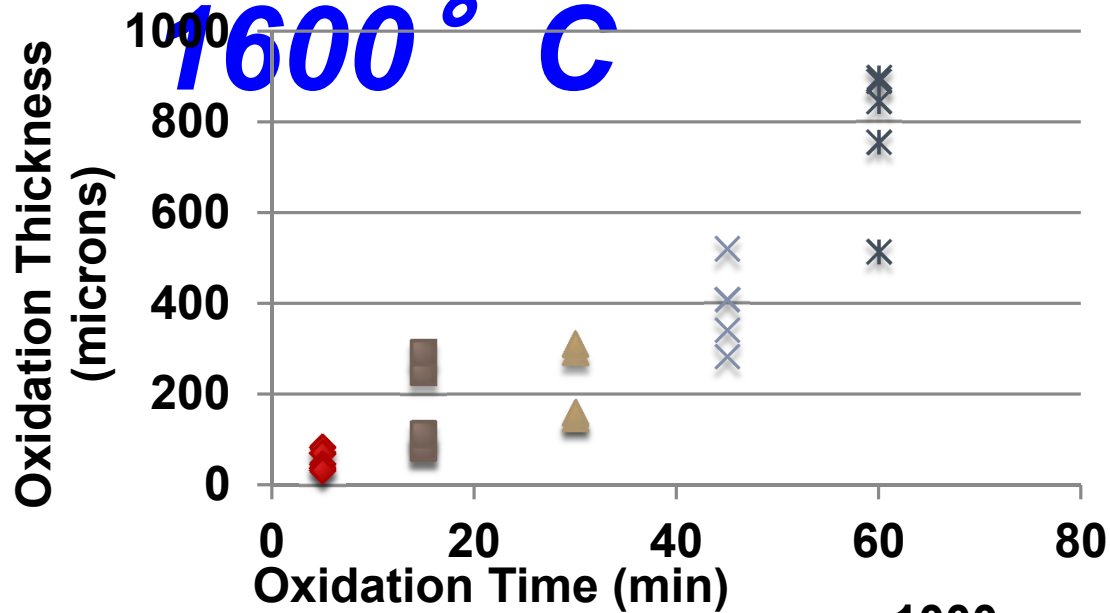
Ti₃AlC core after 30 minute oxidation





Oxidizing Kinetics at

1600 ° C



Extending Previous Kinetic Equations

- Grabke's equations [1965 and 1970] for oxygen transfer on metals (e.g., Fe)

$$\frac{dn_o}{dt} = ka_o^{-m} p_{CO_2} - ka_o^{1-m} p_{CO}$$
- Wang et al. [2003] determined oxidizing sequence for Ti44Al11Nb alloy with X-ray photoelectron spectroscopy.

$$O_2 + 2V = 2O_{ad}$$

$$Al + O_{ad} \rightarrow AlO$$

$$AlO + O_{ad} \rightarrow AlO_2$$

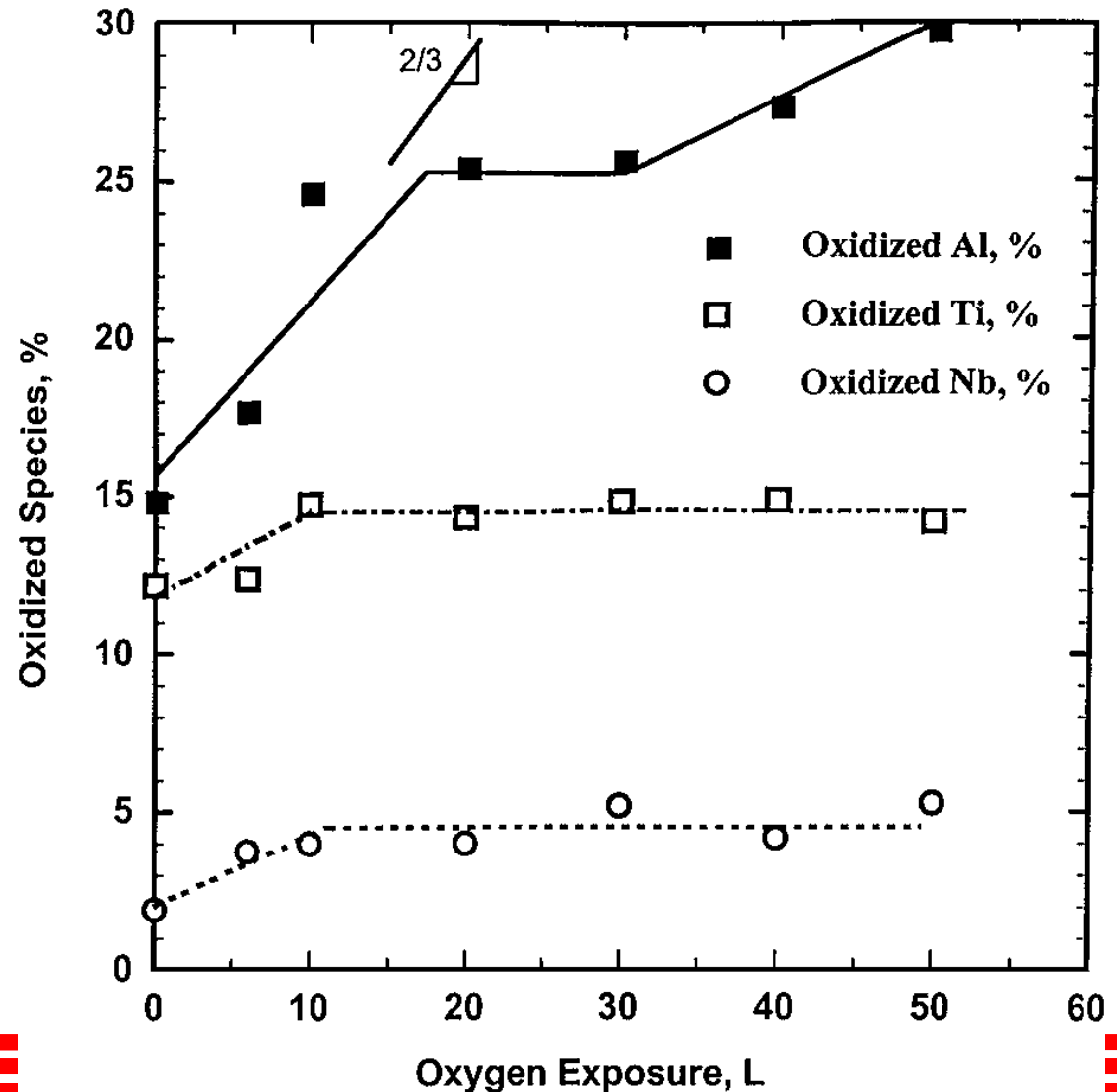
$$AlO_2 + O_{ad} \rightarrow AlO_3$$
- Kurunczi, Guha and Donnelly [2006] on adsorption of oxygen (O_{ads}) on surface sites (V) from O₂ plasma

$$Og + V \rightarrow O_{ads}$$

$$2O_{ads} \rightarrow O_{2(g)} + 2V$$

Oxidized Species Measured on Ti-44Al-11Nb (at%) with X-ray Photoelectron Spectroscopy

- Oxygen exposure of $L = t \cdot p_{O_2}$ (10^{-6} Torr·s)
- Slope of 2/3 acquired from kinetic rates of oxygen adsorption per AlO_3 formation (r_{ad}/r_{AlO_3})



Summary

- Analyzed **thermodynamic stability of oxygen potentials for TiO_x and $\text{TiO}_x\text{-Al}_2\text{O}_3$** for possible scale formation from $\text{Ti}_2\text{AlC-TiC}$ components.
- Used COMSOL, a commercial software package, the temperature profile of a packed bed of B_4C .
- **Controlled oxygen potential** to form $\text{Ti}_3\text{AlC-Al}$ composite which follows parabolic oxidation.
- Examining **the plasma-surface reactions** of the oxidation of Ti-Al-M.
- Determining the effect of **charged surface sites attracting ultimately the oxygen** for surface reactions.





Questions and Comments



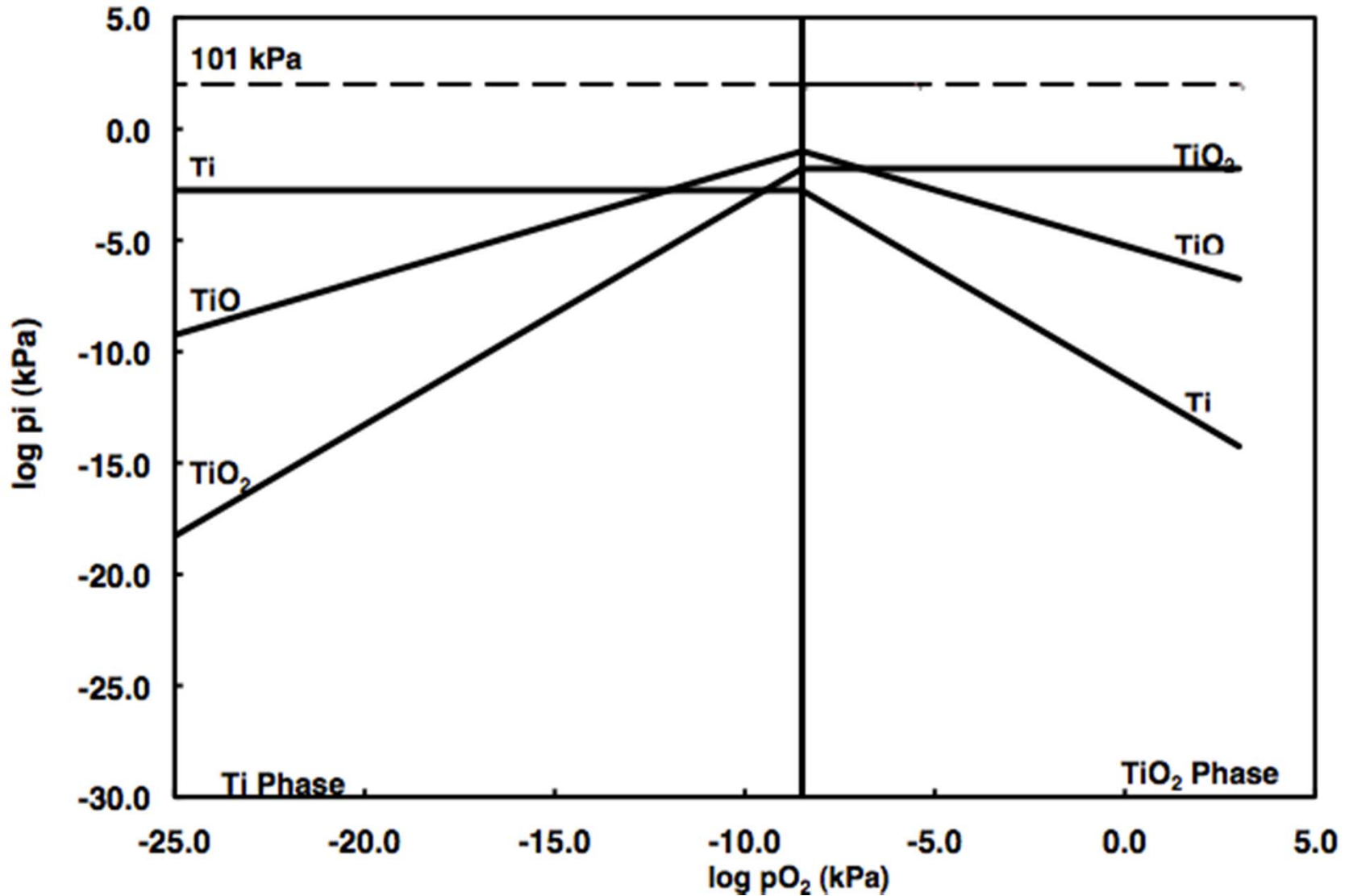


***Slides to Respond to
Possible Queries Follow***



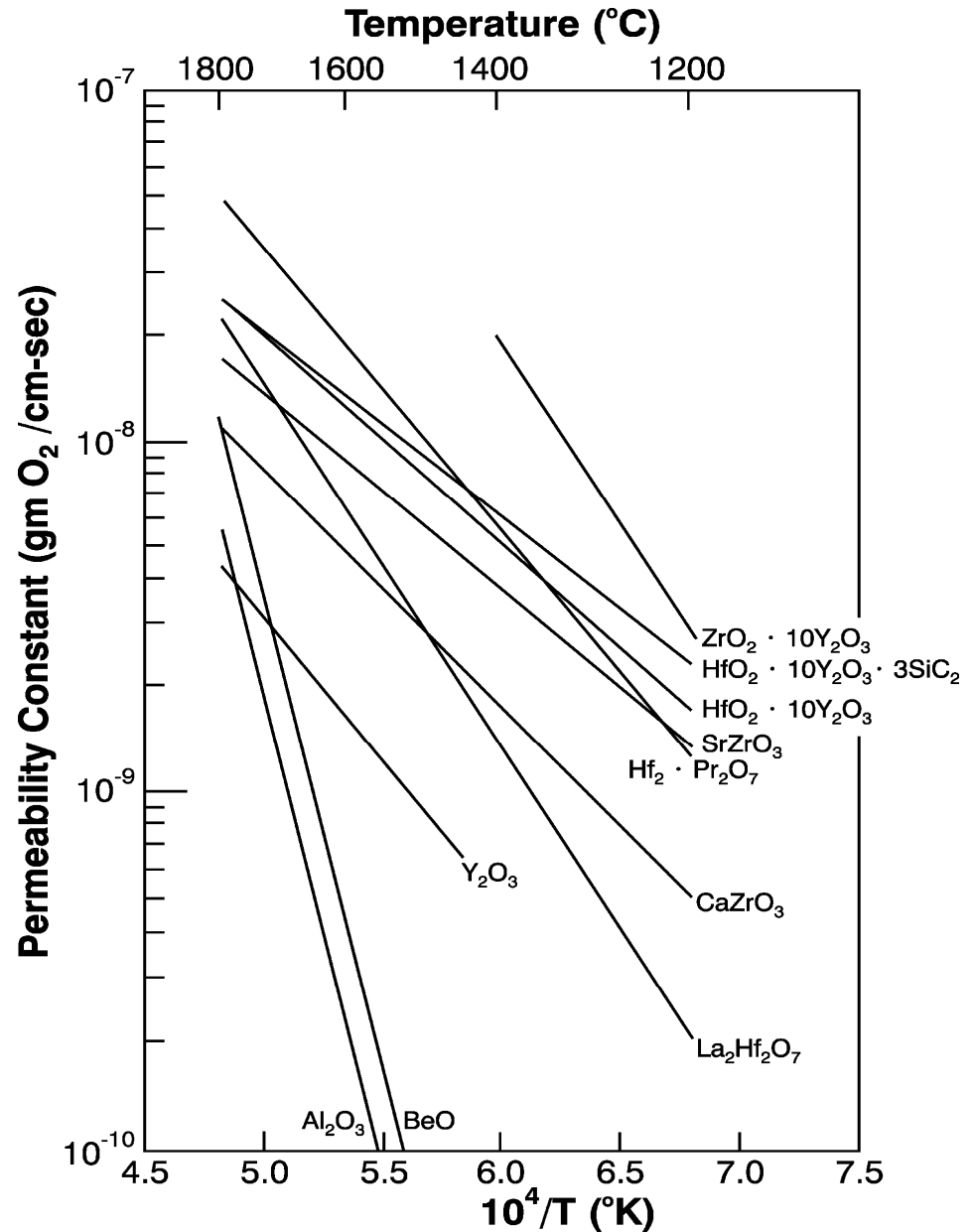


Kellogg Diagram for Ti-O System (2500 K)



Oxygen Permeability

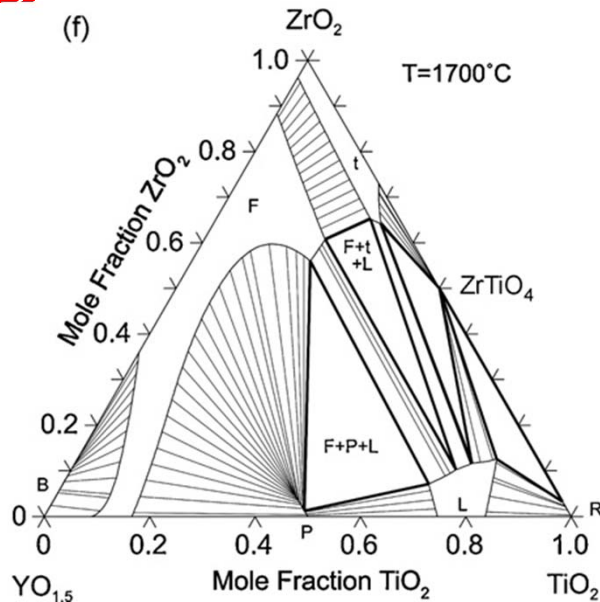
- For temperatures between 1700 to 1500° C Al_2O_3 and Y_2O_3 have oxygen permeability $\leq 10^{-9}$ $\text{gO}_2/(\text{cm}\cdot\text{s})$ and $3\cdot 10^{-9}$ $\text{gO}_2/(\text{cm}\cdot\text{s})$, respectively.
- Oxygen permeability of $\text{ZrO}_2\text{-Y}_2\text{O}_3$ and $\text{HfO}_2\text{-Y}_2\text{O}_3$ increases by approximately an order of magnitude [i.e., $\geq (10)^{-8}$ $\text{gO}_2/(\text{cm}\cdot\text{s})$].



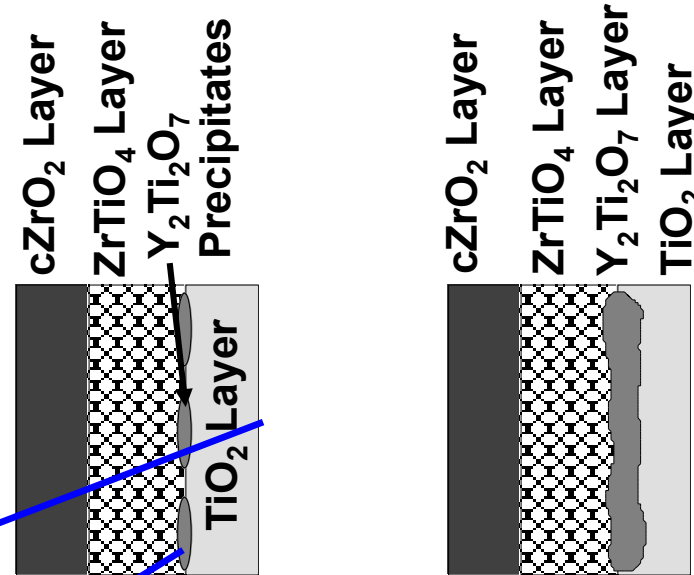
(Opeka, Talmy & Zaykoski-2004)



Wagner's Rate Equation for Scales



Calculated Diagram from Schaedler, Fabrichnaya and Levi -- 2008



$$\frac{1}{A} \frac{d\tilde{n}}{dt} = \frac{1}{\xi} \left[\frac{\tilde{c}}{2} \int_{p_{O_2}^{(i)}}^{p_{O_2}^{(o)}} \left(\left(\frac{z_M}{z_O} \right) D_M + D_O \right) d \ln p_{O_2} \right] = \frac{\tilde{k}}{\xi}$$



Future Efforts for Plasma Surface Reactions

- **Incorporate electron energy** (e.g., electron energy density (n_ε), gradient of electron flux vector (Γ_ε) and potential field (\mathbf{E})).

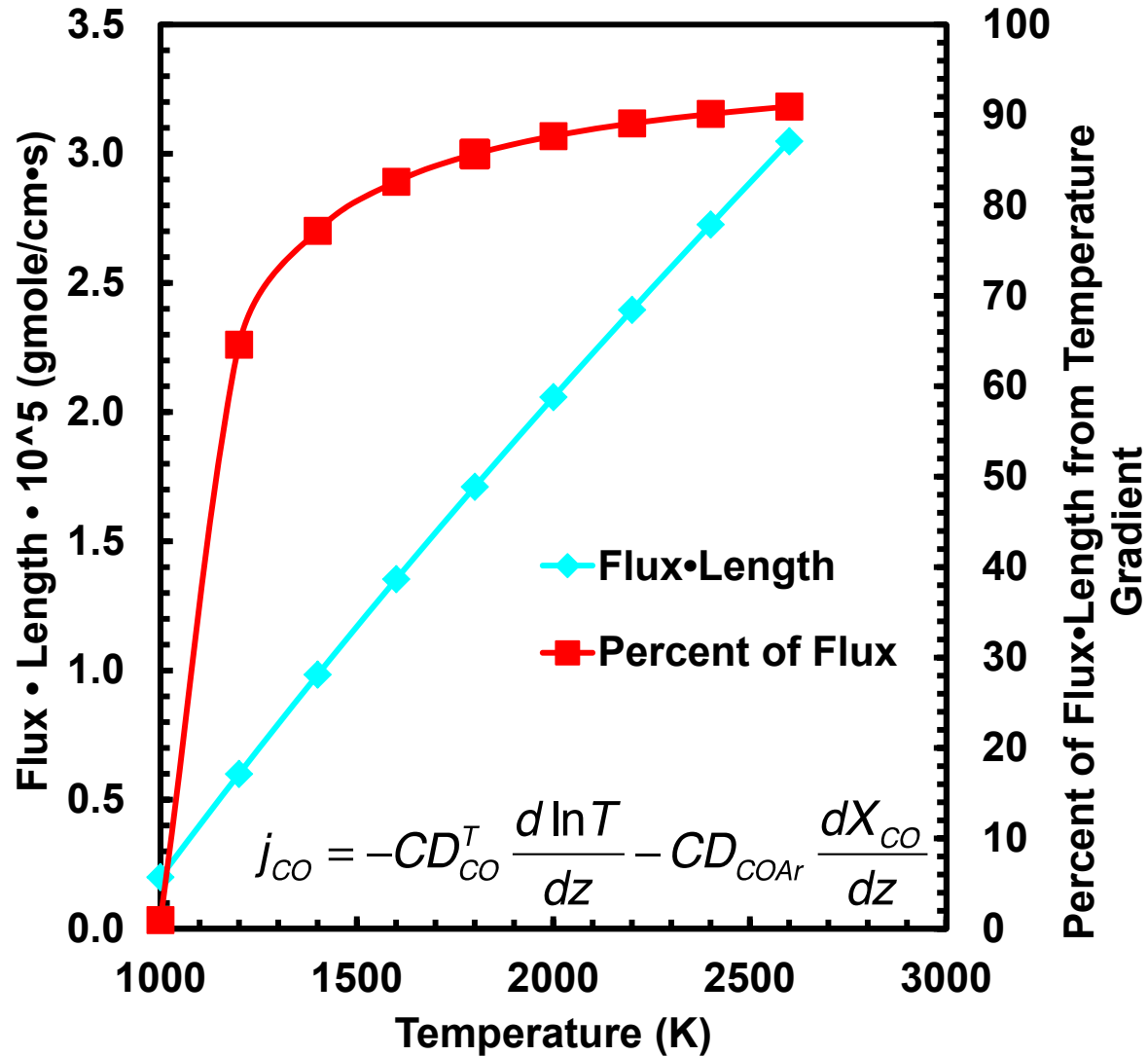
$$\frac{\partial}{\partial t}(n_\varepsilon) + \nabla \cdot \Gamma_\varepsilon + \mathbf{E} \cdot \Gamma_\varepsilon = R_\varepsilon - (\mathbf{u} \cdot \nabla)n_\varepsilon$$

- **Incorporate kinetics of Ar-O₂ plasma-surface reactions** with SiC and Ti₂AlC.
- **Study the effect of temperature extremes** (T and dT/dx) on **metastable phases and/or segregation**.





Diffusional Flux – Kinetics Issues



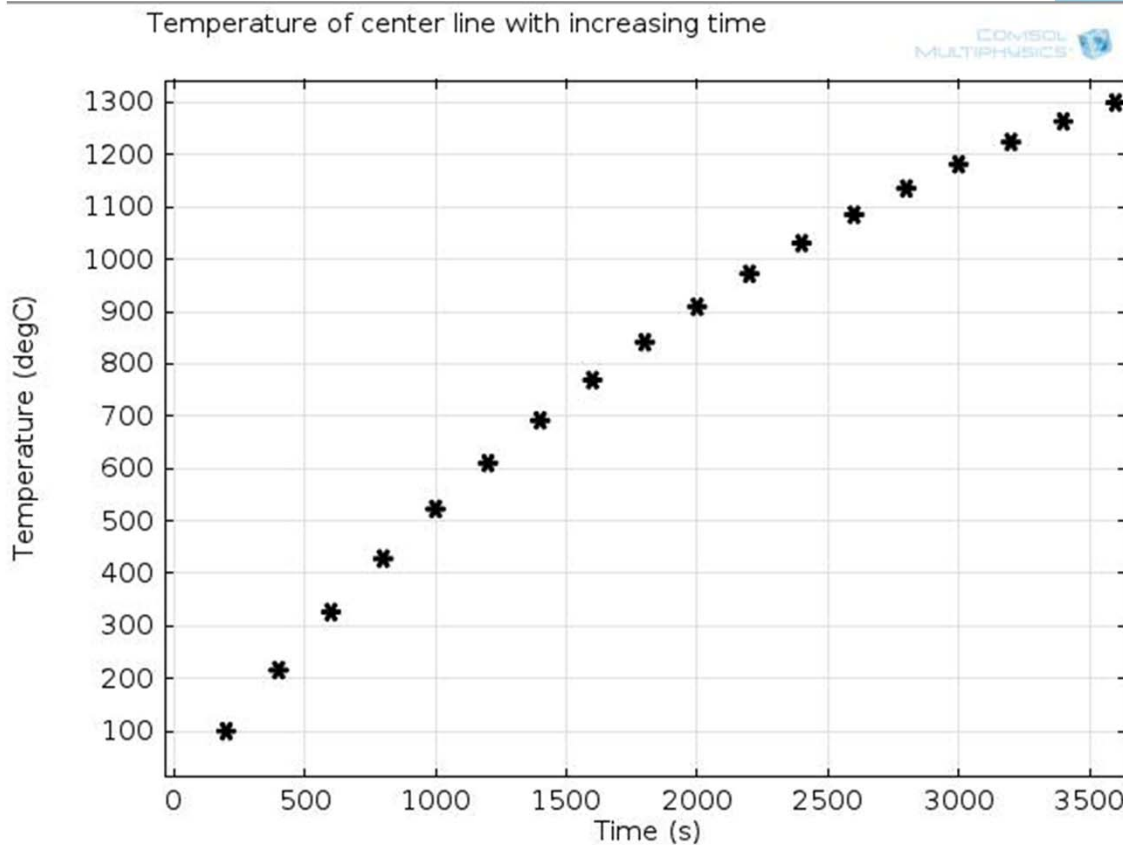
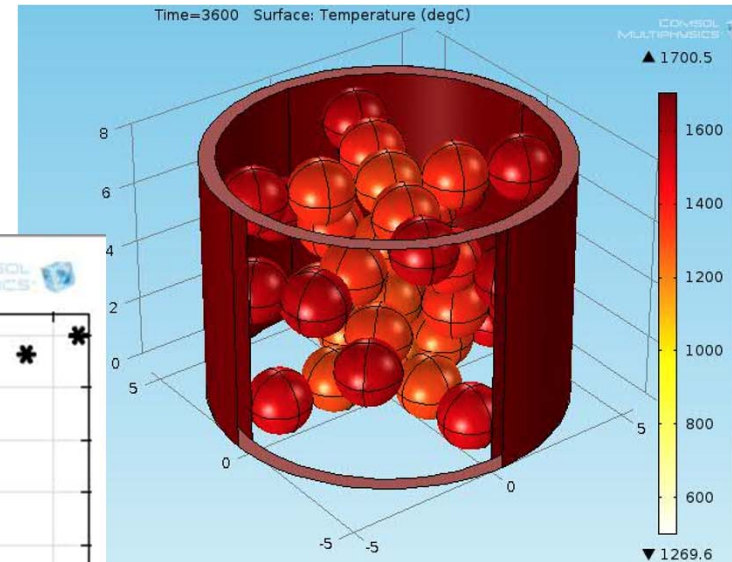
- D_{COAr} from Poirier-Geiger and checked with Chapman-Enskog Eq.
- Mean temperature
$$\frac{T_H T_C}{T_H - T_C} \ln \frac{T_H}{T_C} = 1527K$$
- Al/Al₂O₃/Al₄CO₄ reaction rate?





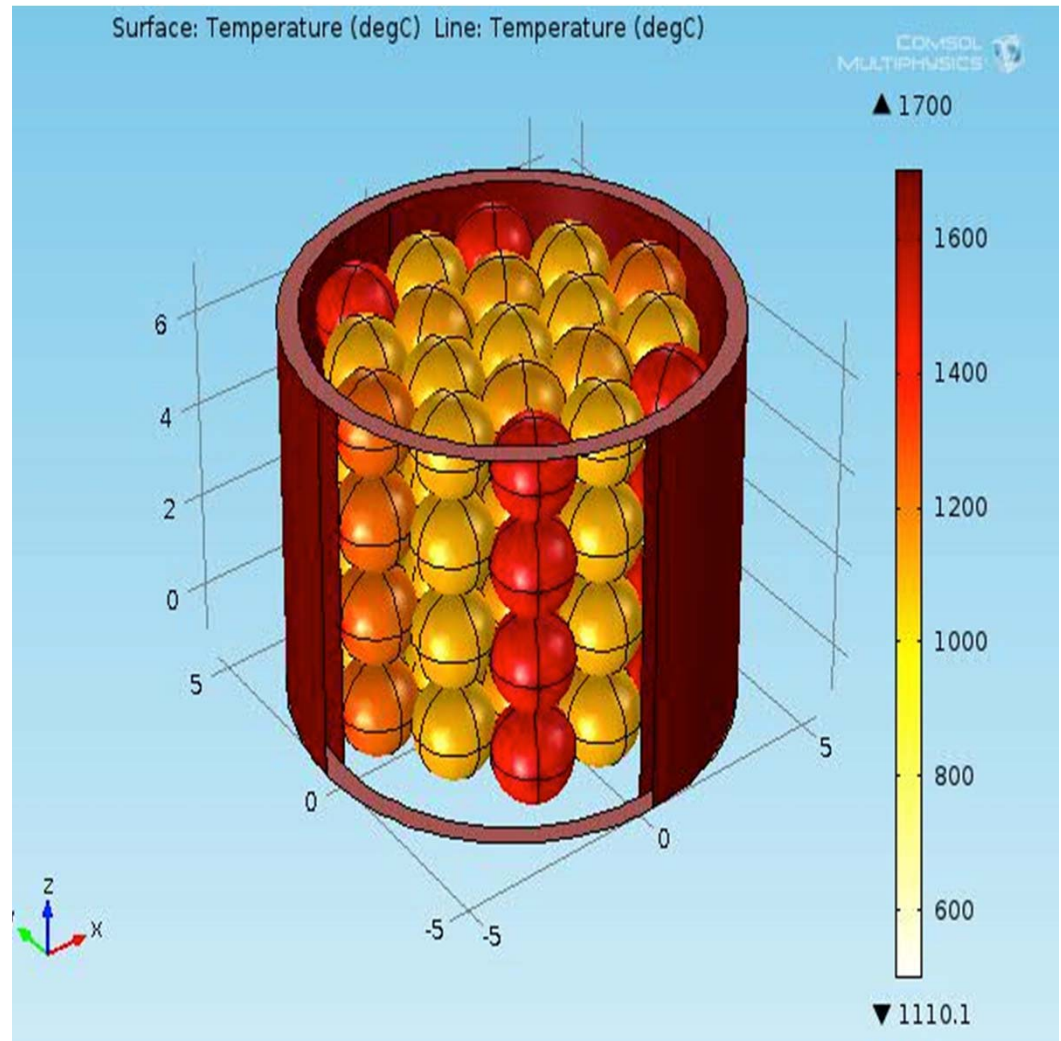
COMSOL Simulation of B_4C Spheres Basis for Packed Bed with Temperature Profile

- Carbide spheres configured in an X-pattern rotating along centerline.
- The spheres have an open structure.



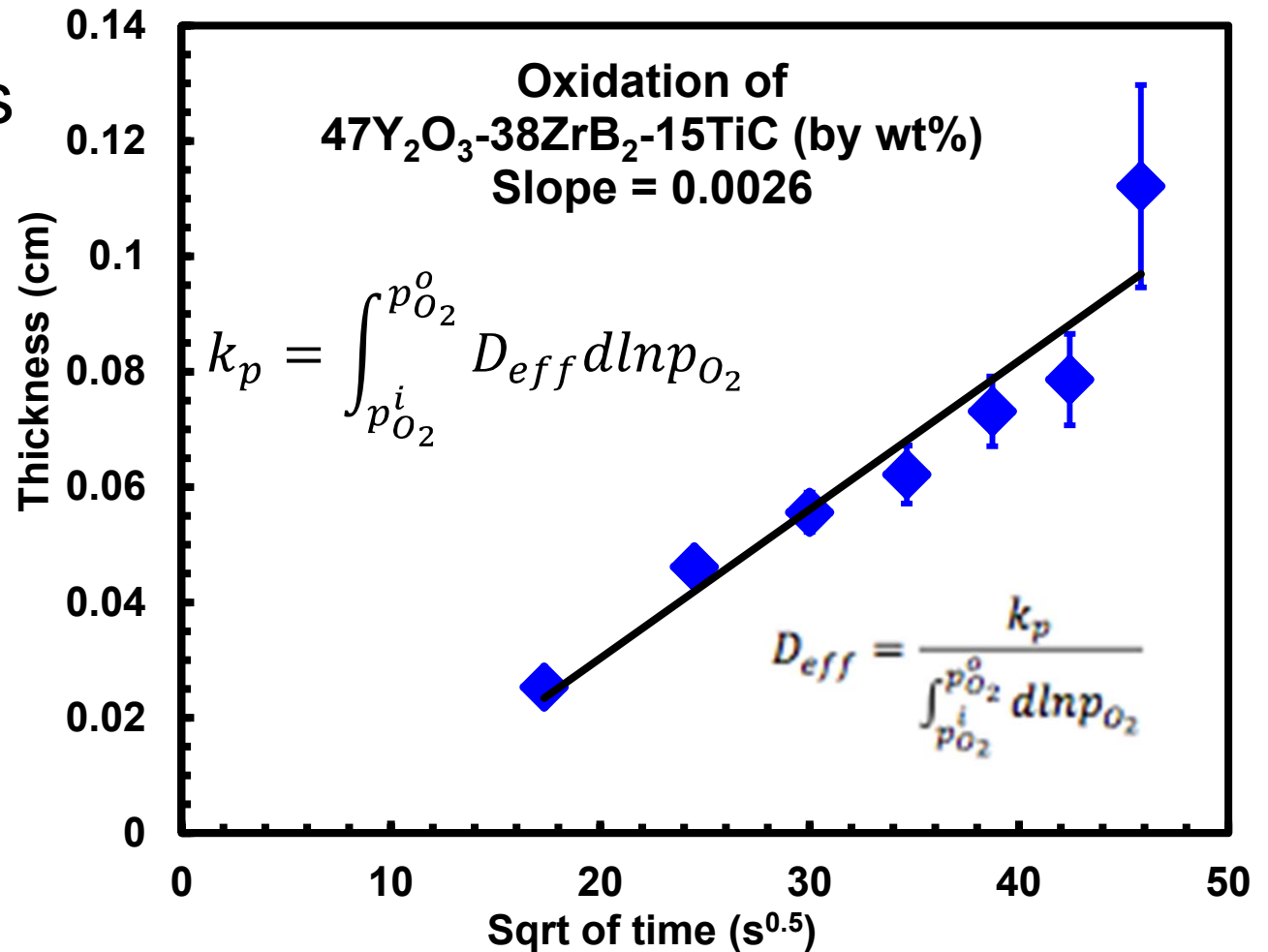
COMSOL Simulation of B_4C spheres in a packed bed

- Cylindrical graphite wall temperature is heated mimicking internal furnace wall.
- Carbide spheres touch each other with a 6-fold lateral configuration though each layer contacts uniformly.
- Spheres contacting the wall have highest temperature.
- Conductive heat transfer was used, but radiation will be added with expanded sphere number.



Parabolic Growth Rate of Scale

- $D_{\text{eff}} = 10^{-11} \text{m}^2/\text{s}$ for t-ZrO₂-Y₂O₃ phase as controlling layer



Electron-Energy Transport

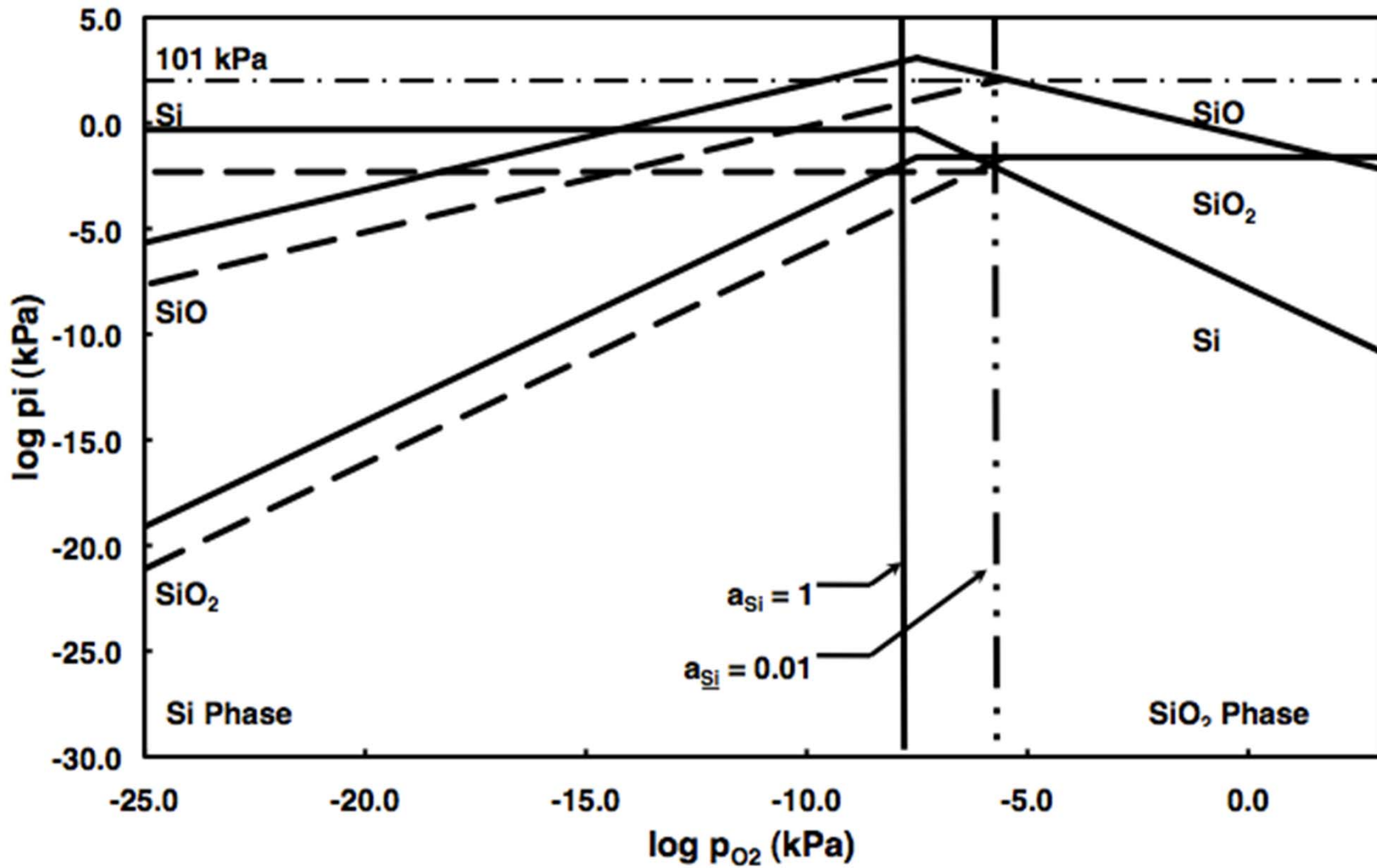
- Should consider electron, ions and neutral species balance coupled with electron energy and momentum balances.

$$\frac{\partial}{\partial t} (n_{\varepsilon}) + \nabla \cdot \Gamma_{\varepsilon} + \mathbf{E} \cdot \Gamma_{\varepsilon} = R_{\varepsilon} - (\mathbf{u} \cdot \nabla) n_{\varepsilon}$$

$$\frac{\partial}{\partial t} (n_e) + \nabla \cdot [-n_e(\mu_e \cdot \mathbf{E}) - \mathbf{D}_e \cdot \nabla n_e] = R_e$$

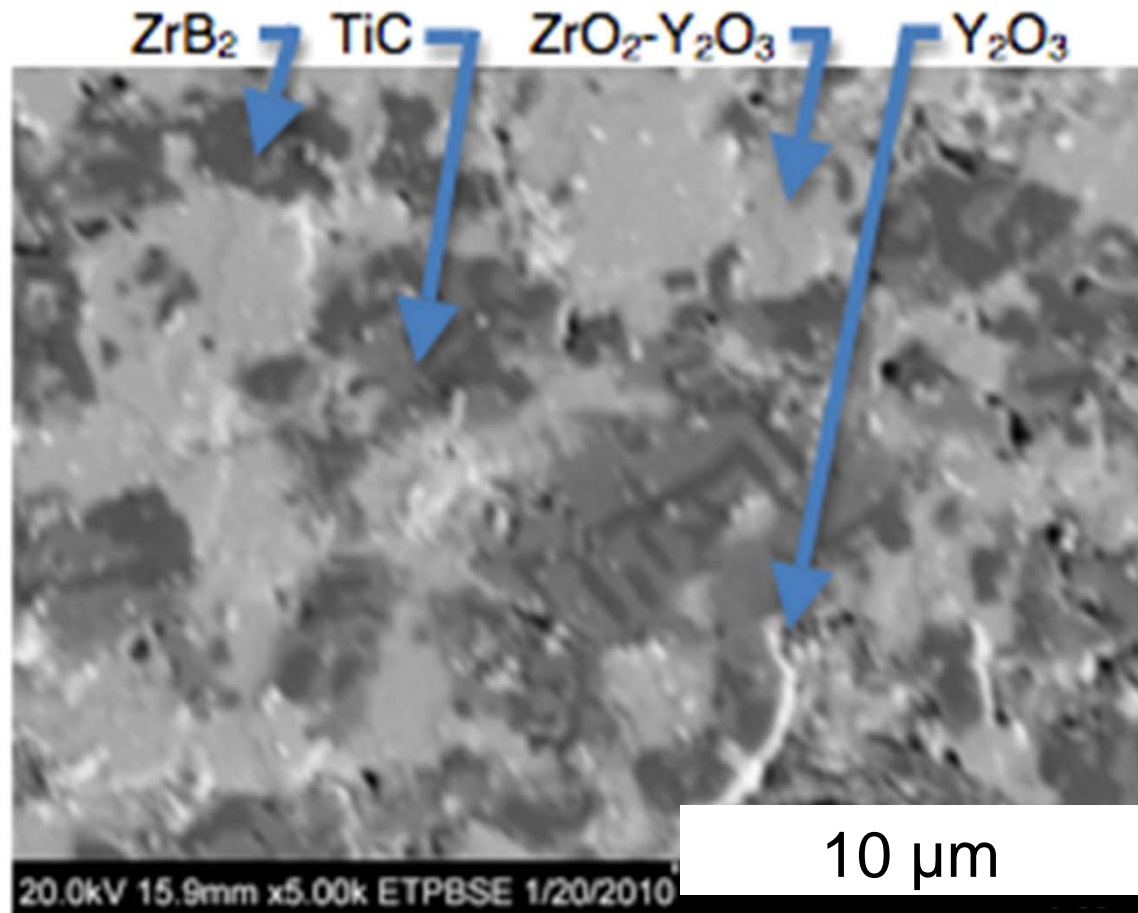


Kellogg Diagram for Si-O System (2500 K)



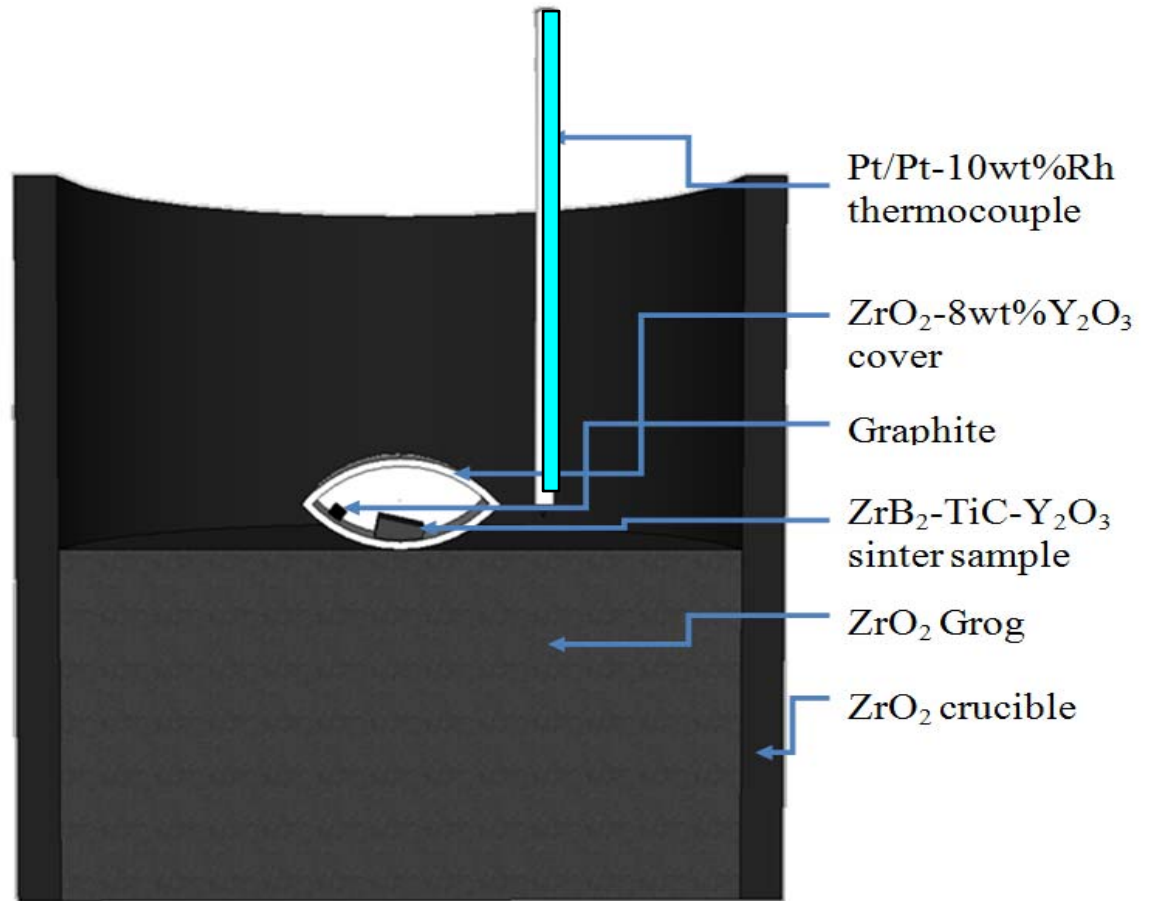
SEM image after spark-plasma sintering

- ZrB_2 oxidizes to ZrO_2 dissolving some Y_2O_3
- Stringers of Y_2O_3 appear in grain boundary
- Graphite seems to minimize TiC oxidation.



Oxidation in Silicide Furnace with air and C/CO/N₂ atmospheres at 1700° C

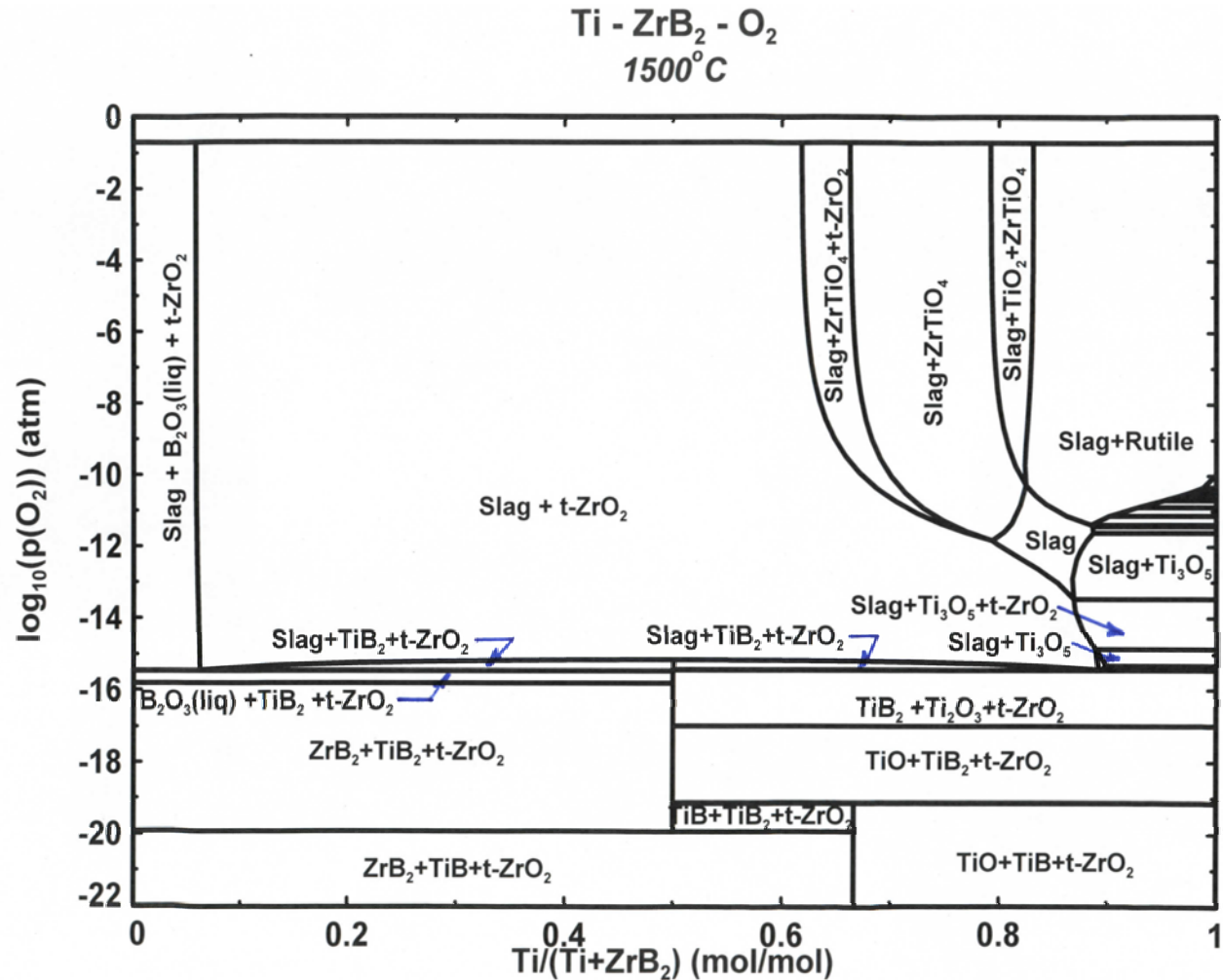
- Spark plasma-sintered samples
- ZrO₂-8 wt% Y₂O₃ crucible covers were used to hold samples.
- Hf foil were also used to hold samples.





Oxygen Levels for TiO_x with Calculated $Ti-ZrB_2-O_2$ Phase Diagram

- Ti oxides start to form near $p_{O_2} > 10^{-22}$ atm with TiO.
- Ti_2O_3/Ti_3O_5 has $p_{O_2} = 10^{-15.5}$ atm
- ZrB_2 oxidizes to t- ZrO_2 with Ti oxides.
- Liquid oxides form with increasing p_{O_2}





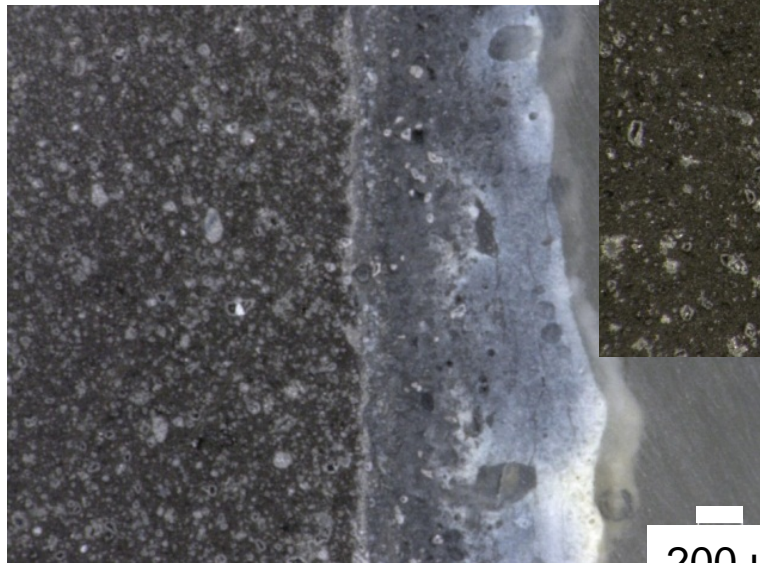
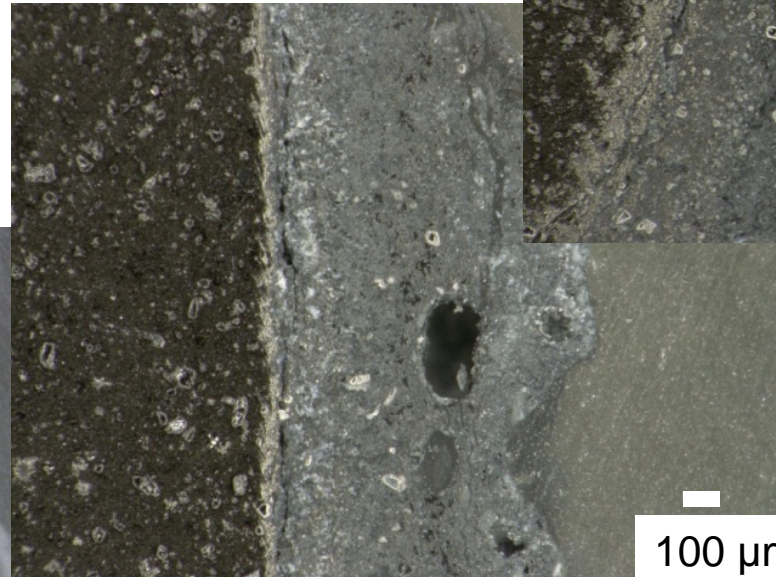
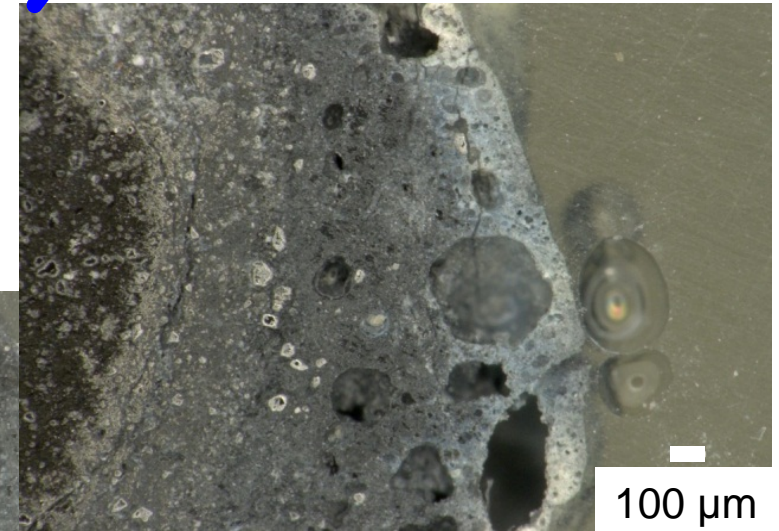
Optical Microstructures to Measure Scale

35 minutes

Increasing Oxidizing Time

20 minutes

30 minutes



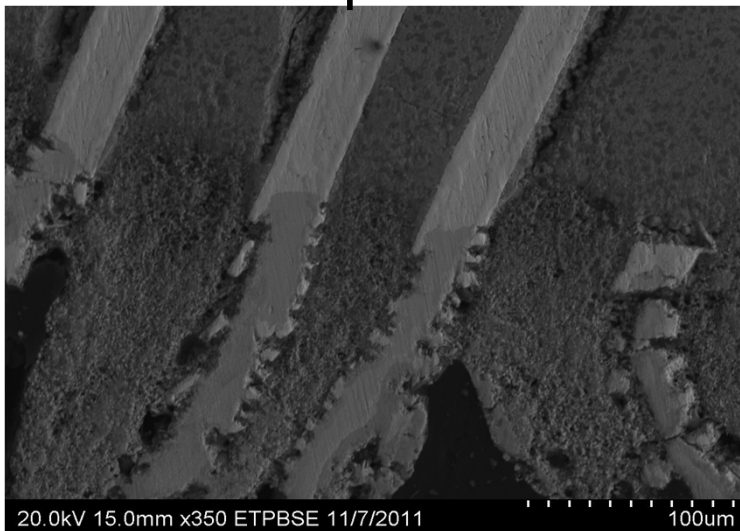
200 μm



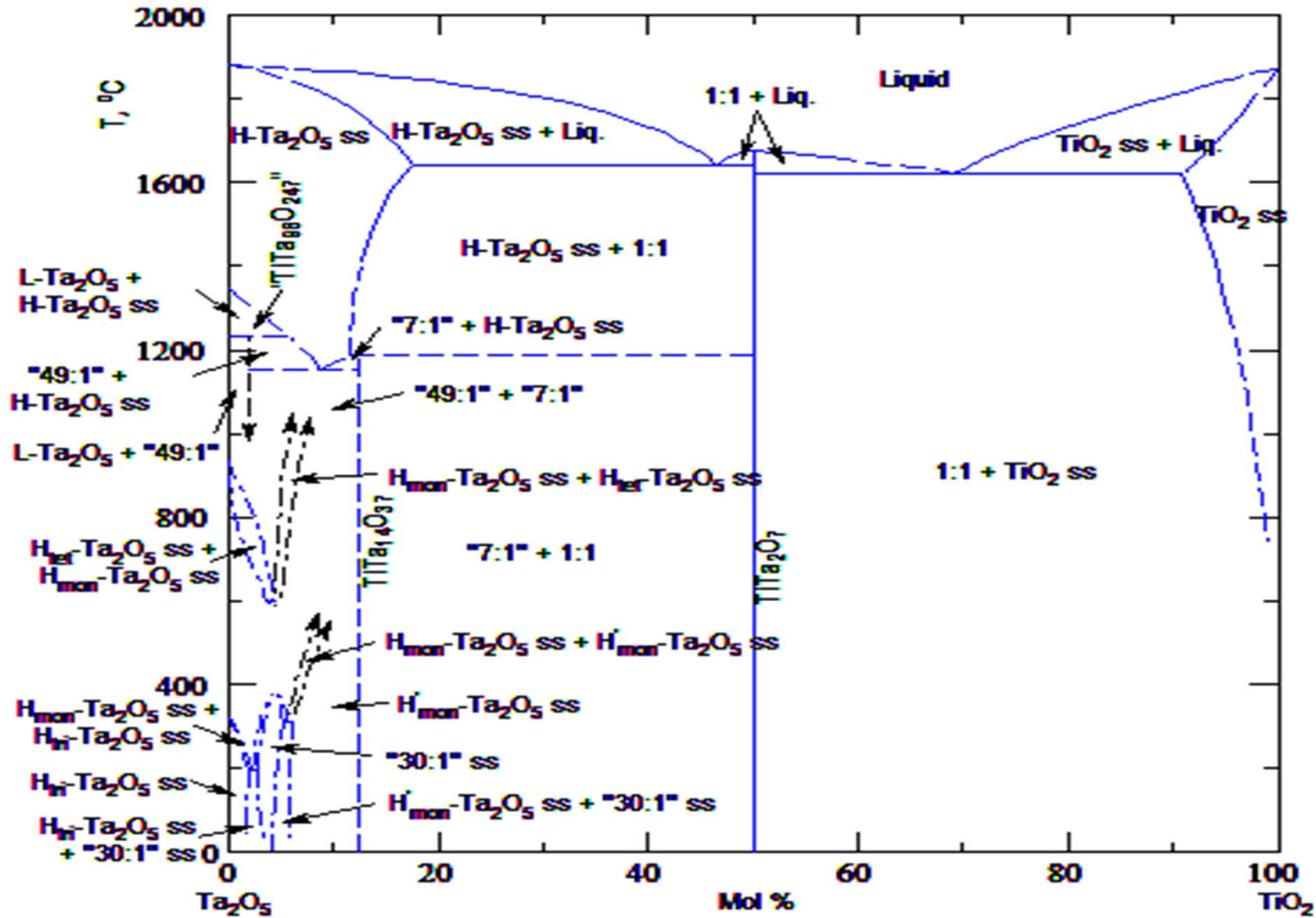
Oxidized 30ZrB₂-13TiC-37Y₂O₃-20Ta sample for 3 minutes at 1700° C

- Oxidized area becomes ZrO₂-TiO₂-Y₂O₃
- Ta forms Ta₂O₅ upon oxidation with vaporization

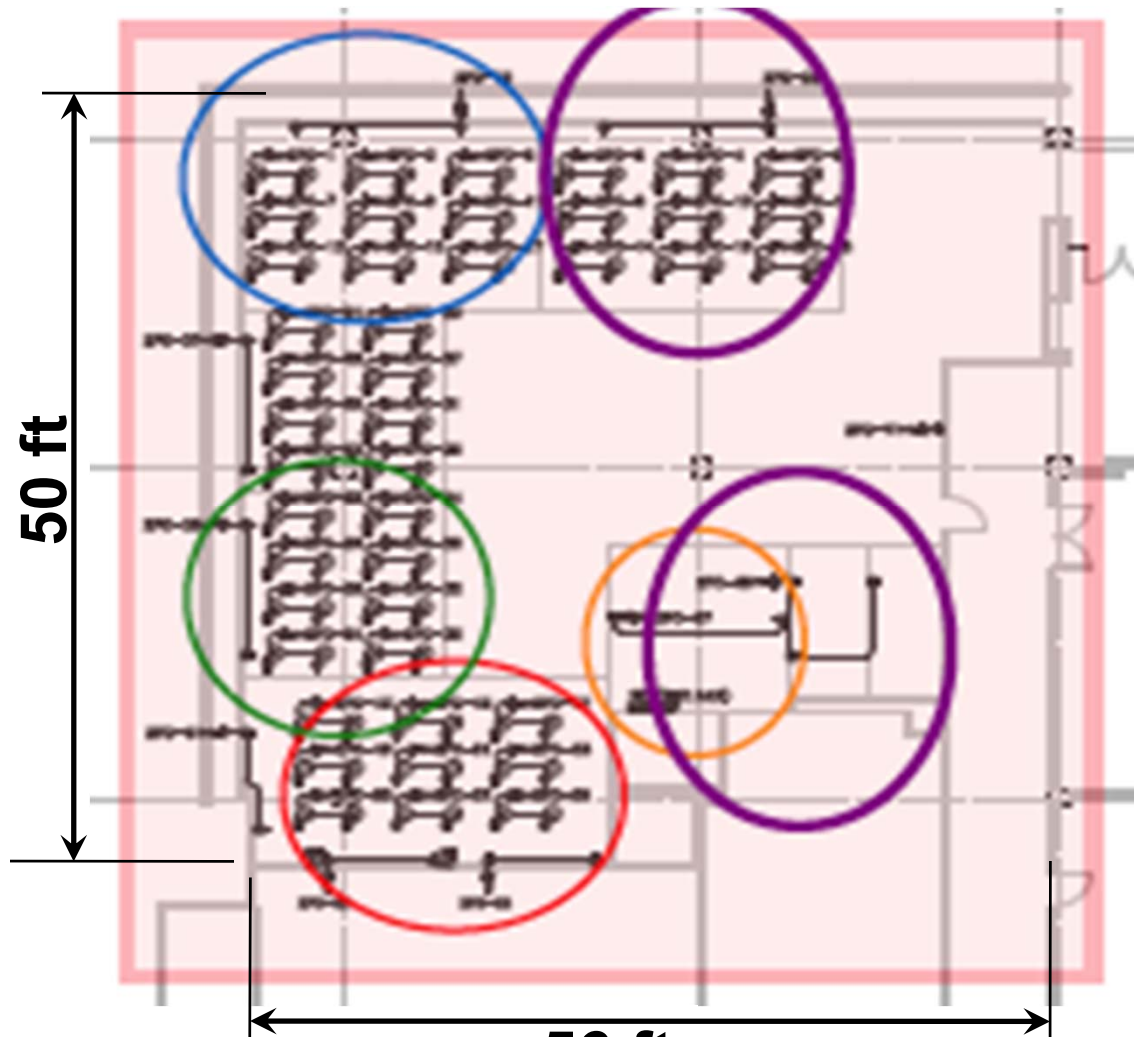
Oxidized Area
Ta ZrB₂-TiC-Y₂O₃ matrix



Ta₂O₅-TiO₂ phase diagram



Remodeling Departmental Materials and Structures Laboratory (Dynamic)

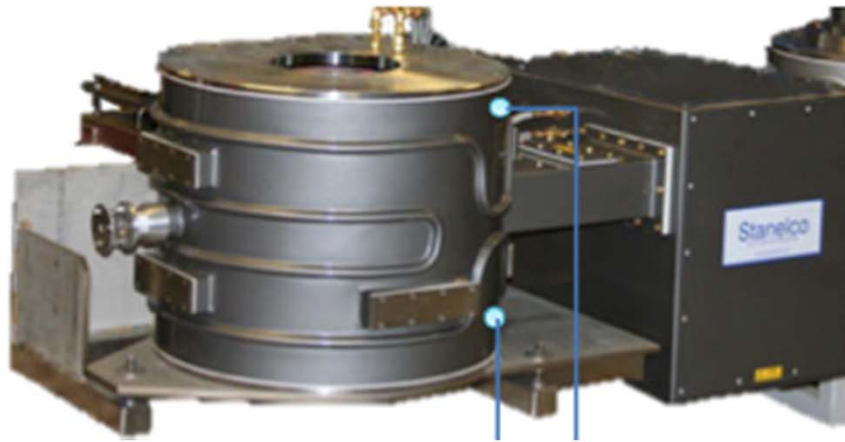


- Other than standard 120VAC, will need:3-phase,
- 480 VAC in Bay 2 (encircled - blue)120A,
- 3-Phase, 240VAC in Bay 4 (encircled - green) 40A,
- Single Phase, 210VAC in Bay 5 (encircled - red)50A,
- 3-Phase, 240VAC in Bay 5 (encircled - red)50A,
- 3-Phase, 240VAC in Bay 6 (orange) Purple Area .

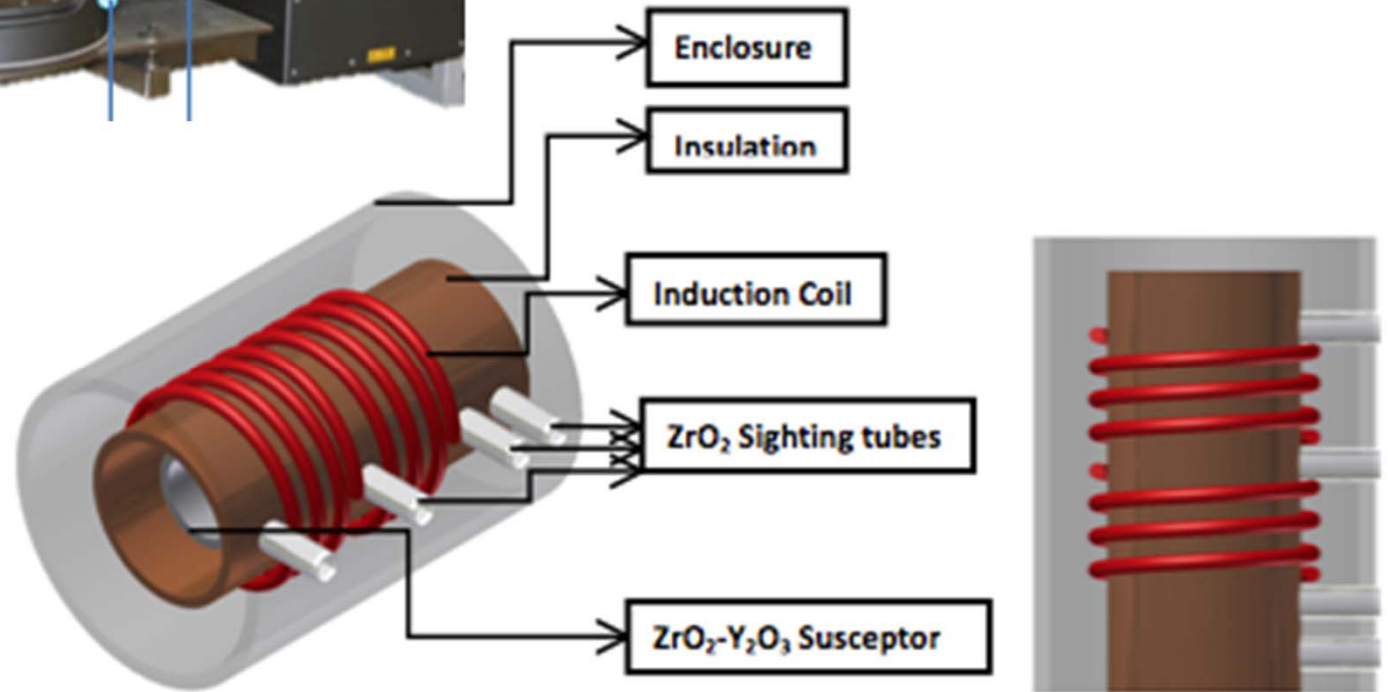
56 ft



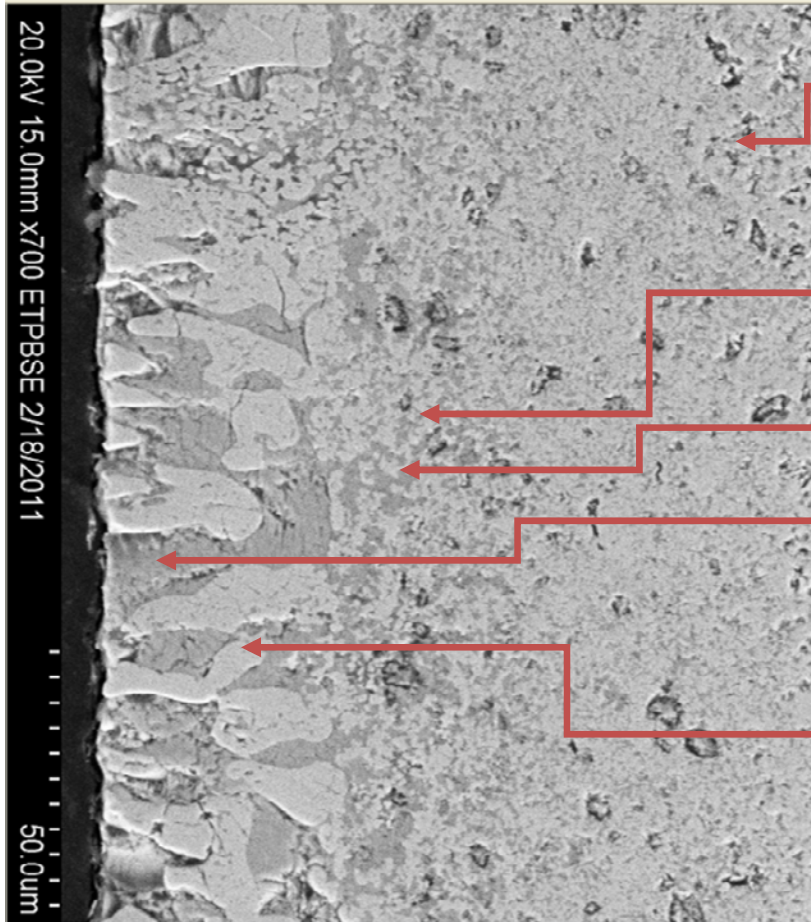
Seek DURIP Request for Ultra-high Temperature Furnace



- Dielectric induction furnace (3-7 MHz) reaching 2600 or 3500° C
- Four Infrared pyrometers
- Support AFOSR/ONR efforts



Phases identified for oxidized sample in C/CO/N₂



ZrB₂-TiC-
Y₂O₃

Y₂O₃

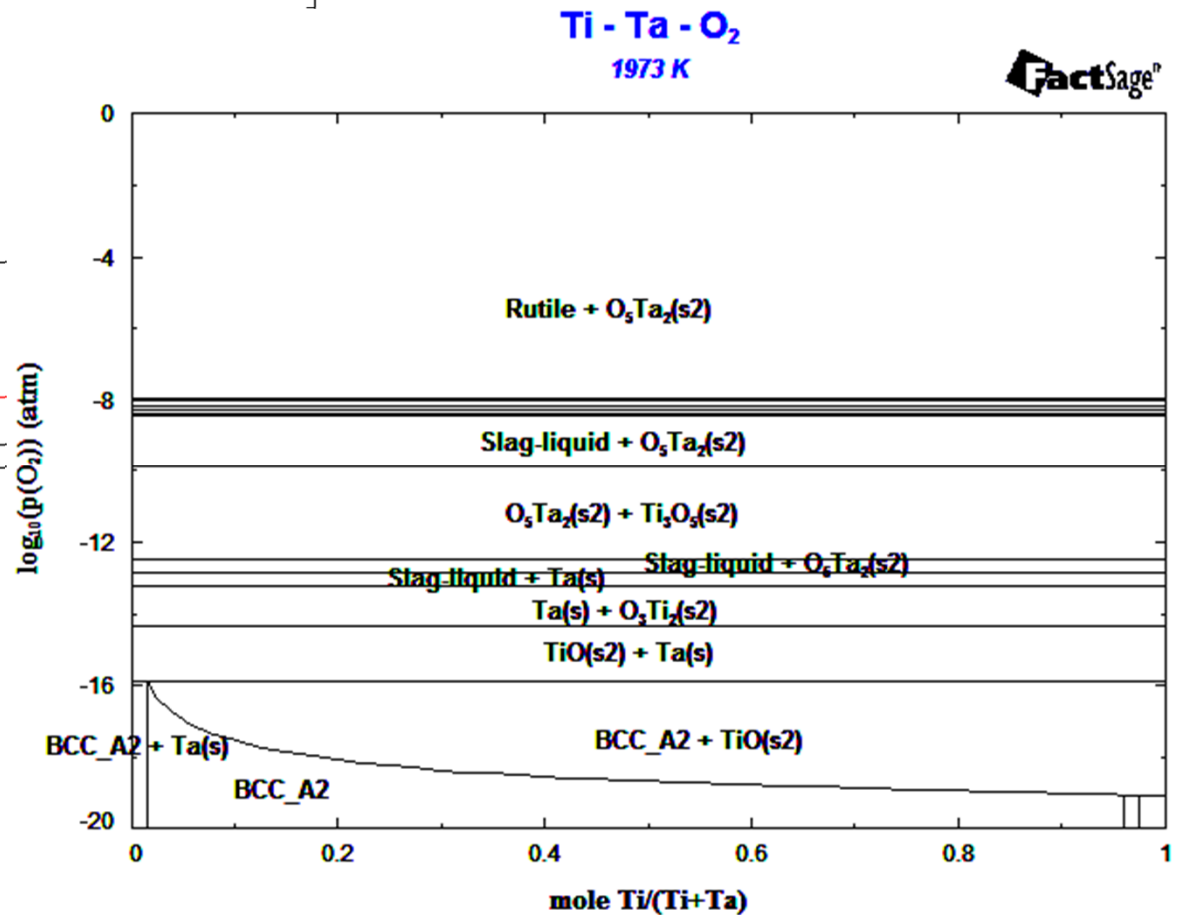
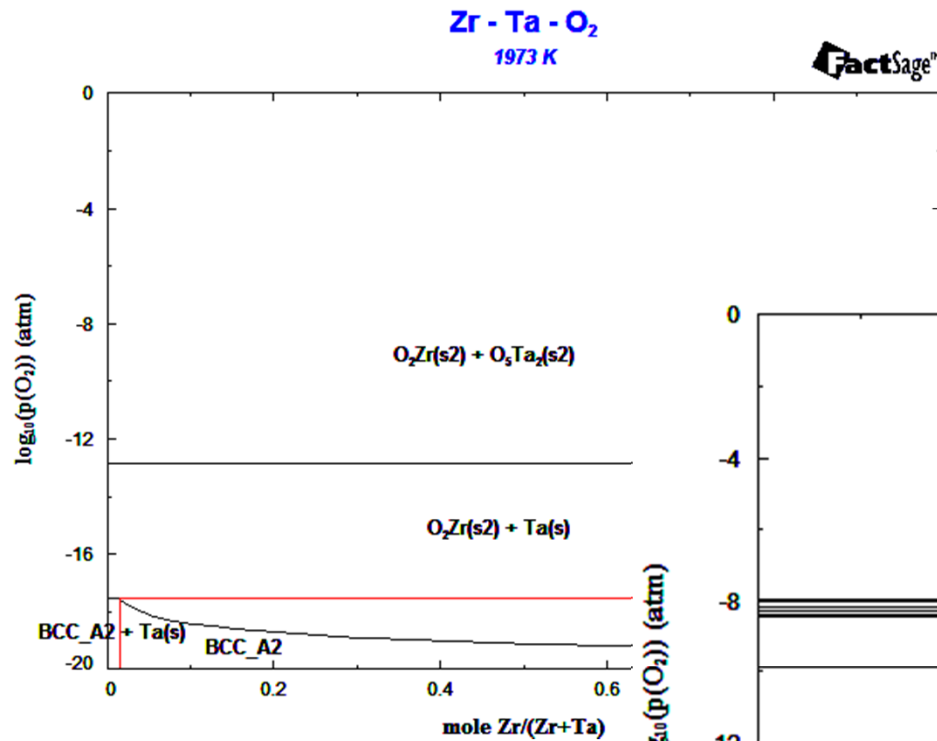
ZrO₂-TiO₂-Y₂O₃

Y₂O₃

ZrO₂



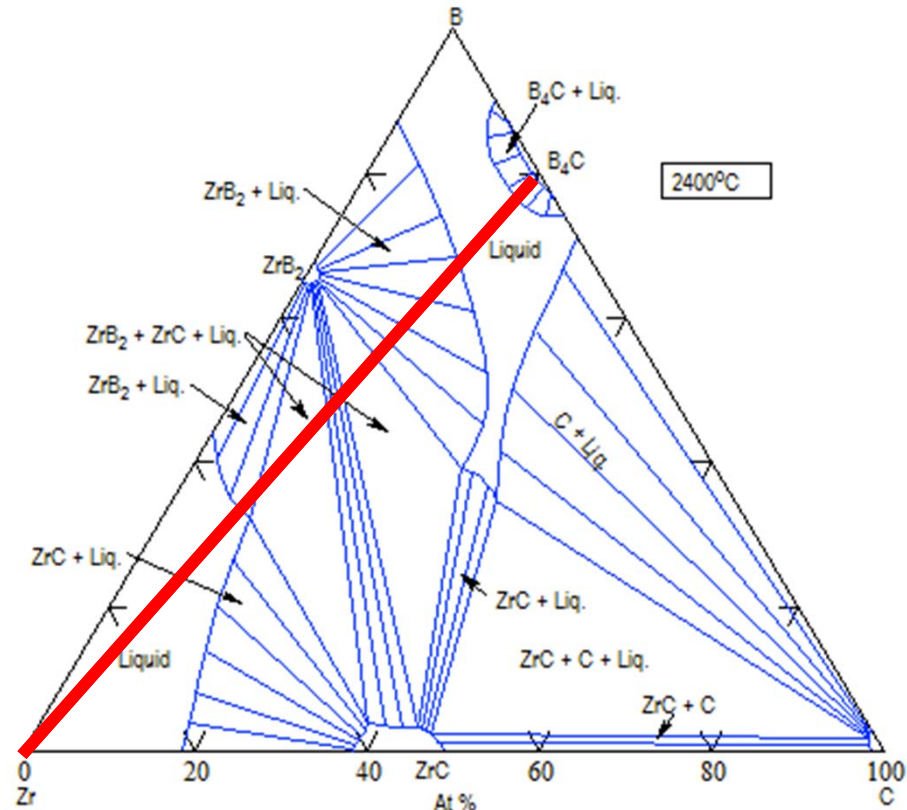
Calculated Zr-Ta-O₂ and Ti-Ta-O₂ phase diagrams



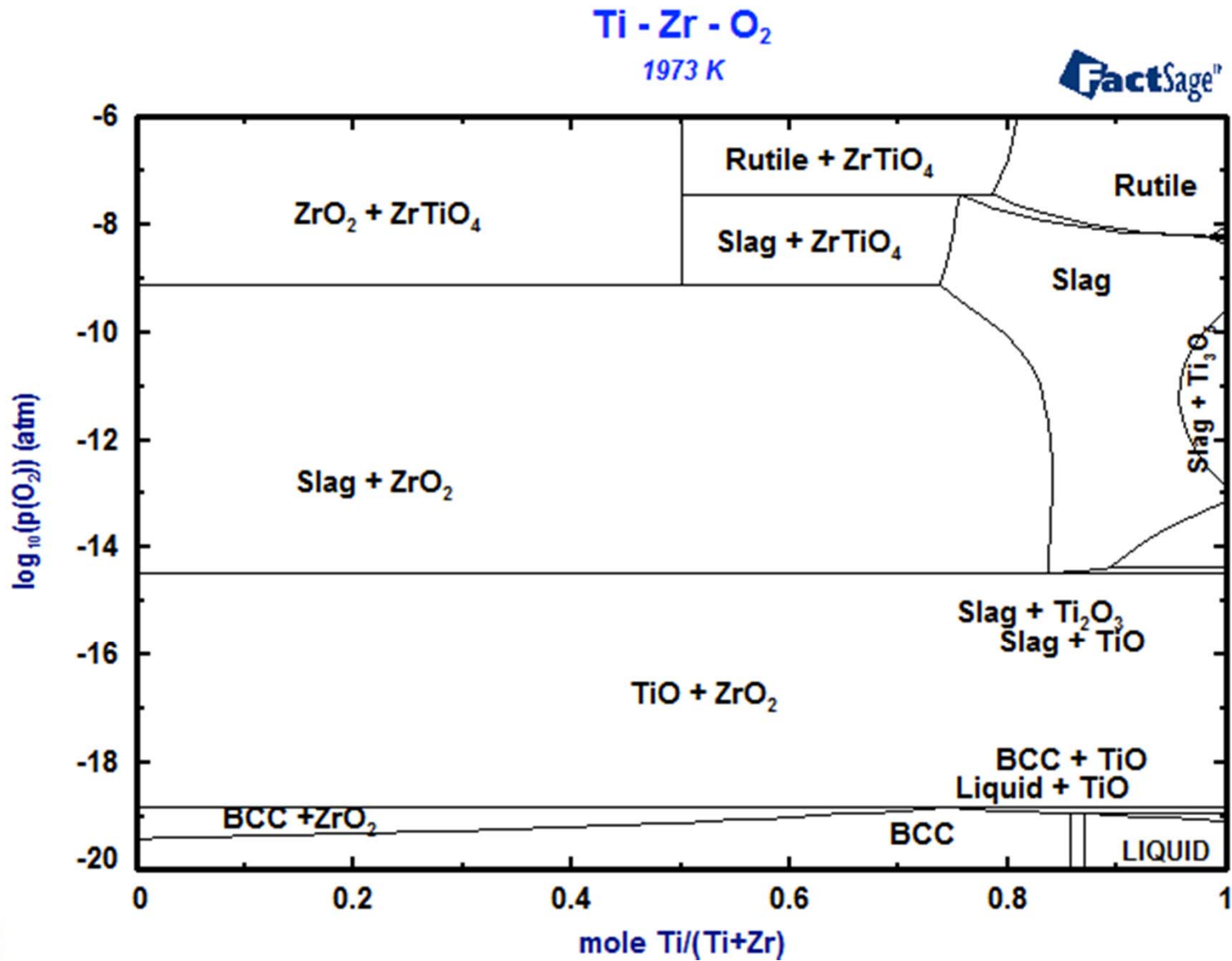
- p_{O₂} level for Ta/Ta₂O₅
- TiO_x-Ta₂O₅ liquids

Zr as primary component in B_4C reaction on Zr-B-C phase diagram

- Zr liquid changes with alloy composition
- Zr reacts with B_4C forming ZrC and ZrB_2 as a result of the mass balance.

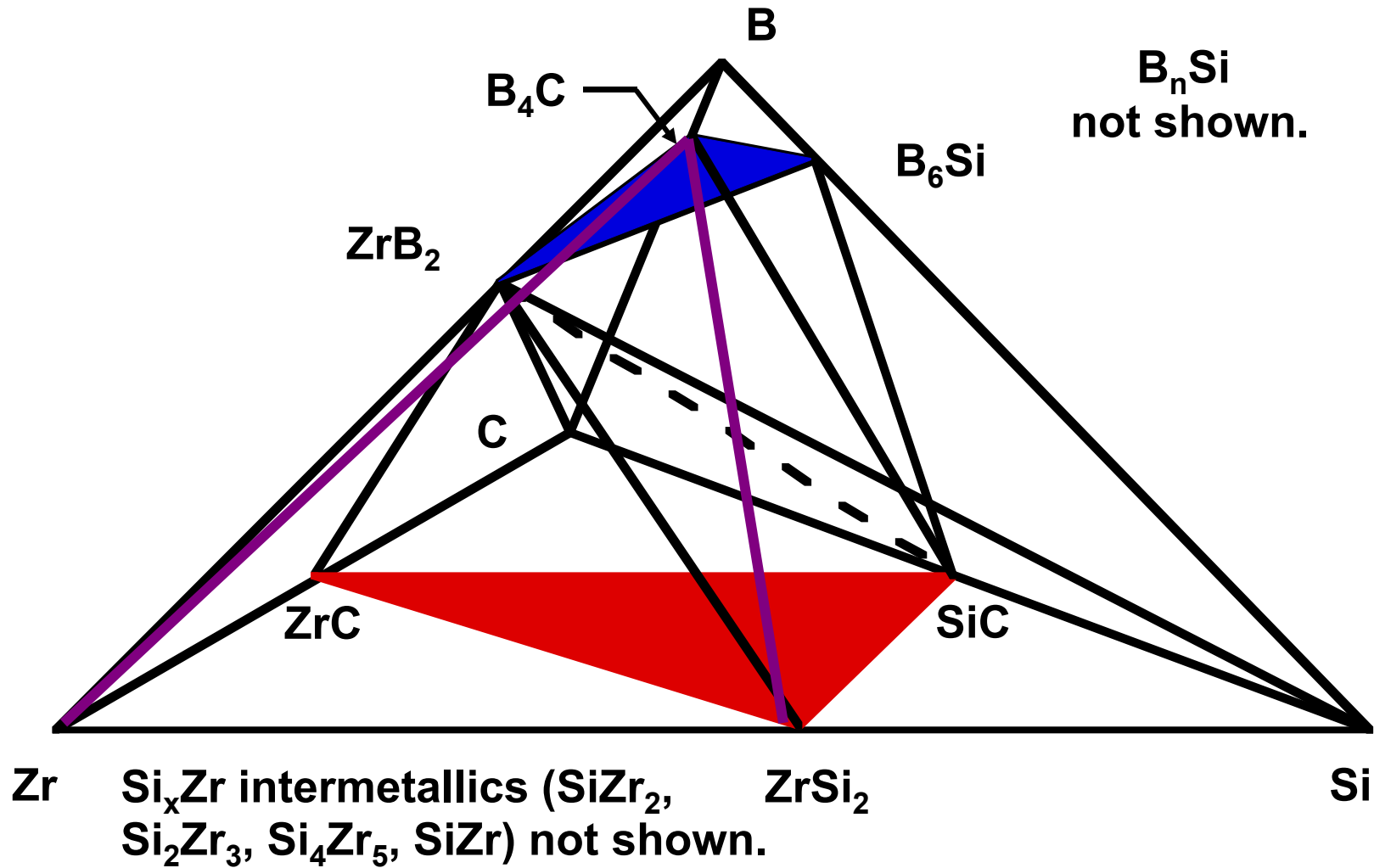


Ti-Zr-O₂ Phase Diagram at 1973 K



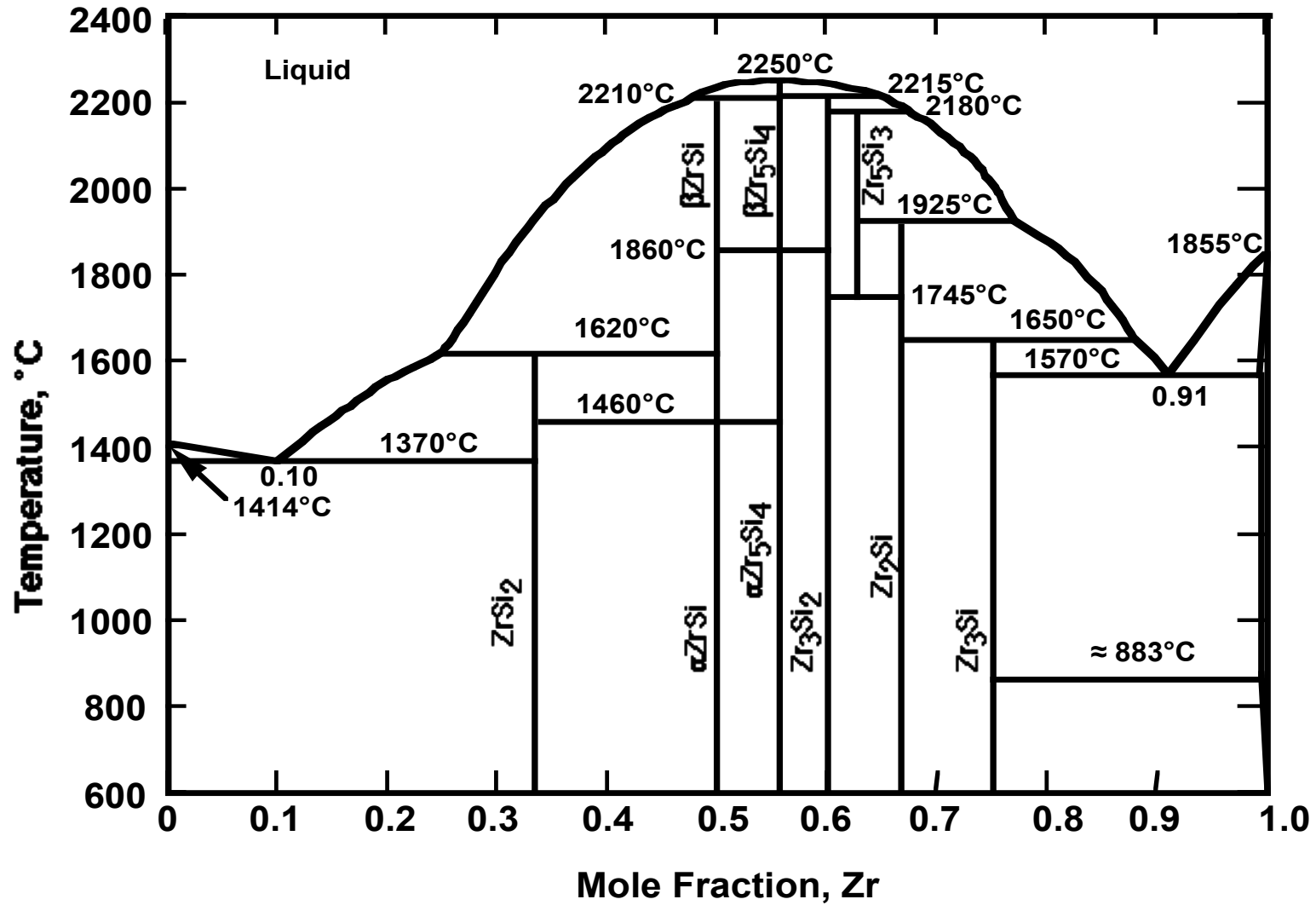


Zr-C-B-Si Quaternary (Proposed by Sorrell-1993)



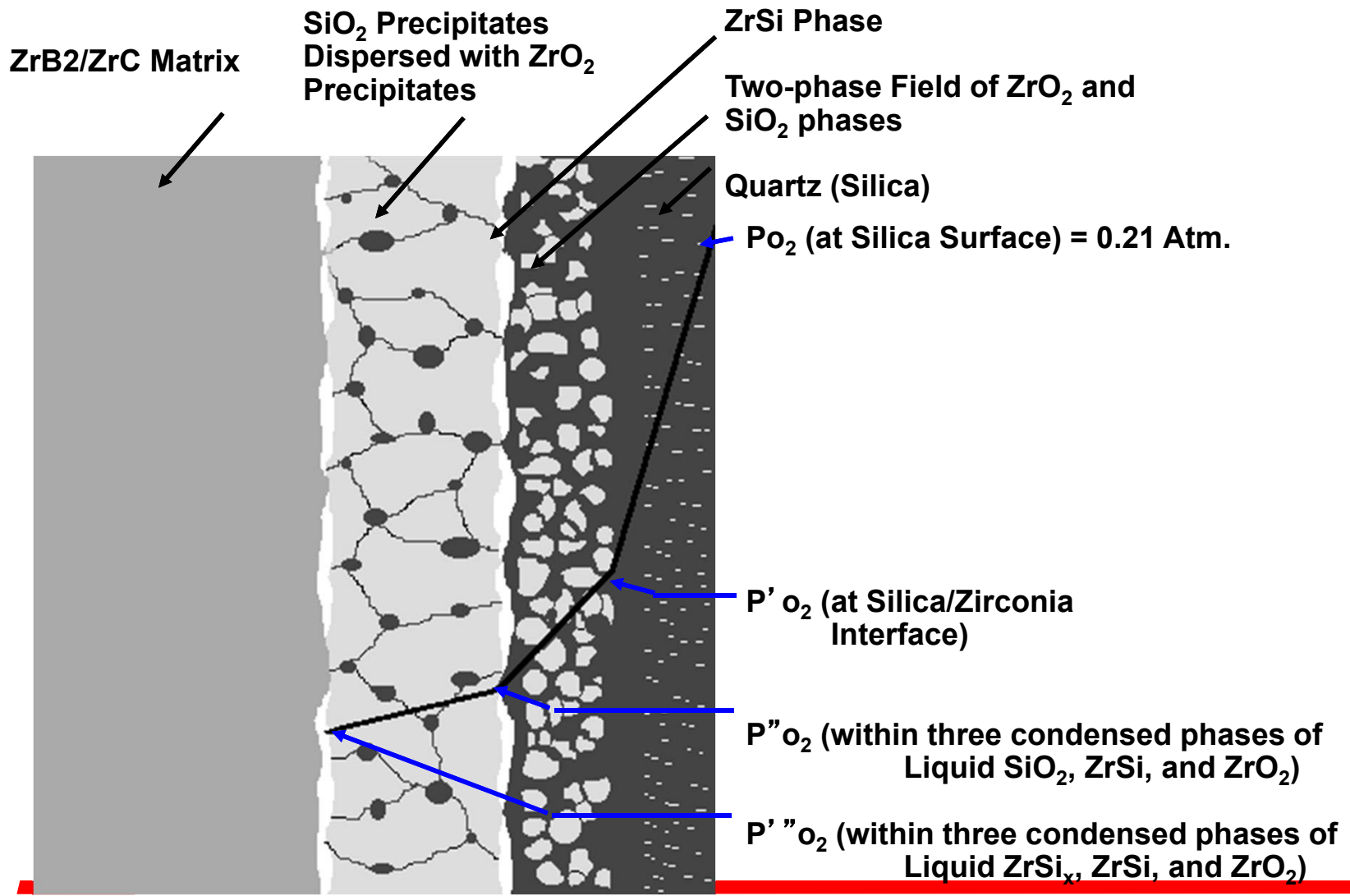


Zr-Si Phase Diagram





Oxygen Partial Pressure Gradient

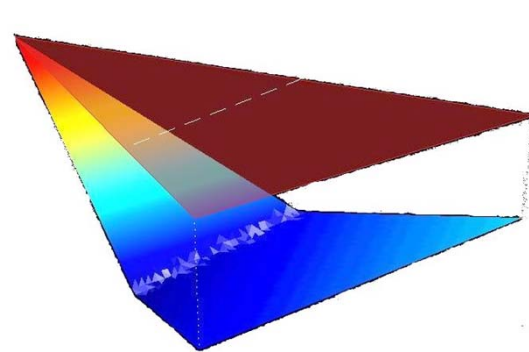
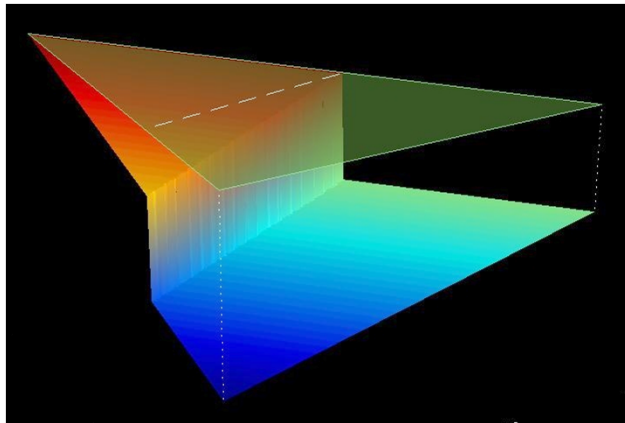


X-FEM Basics

- Extend finite element approximation space to reproduce “difficult” functions.

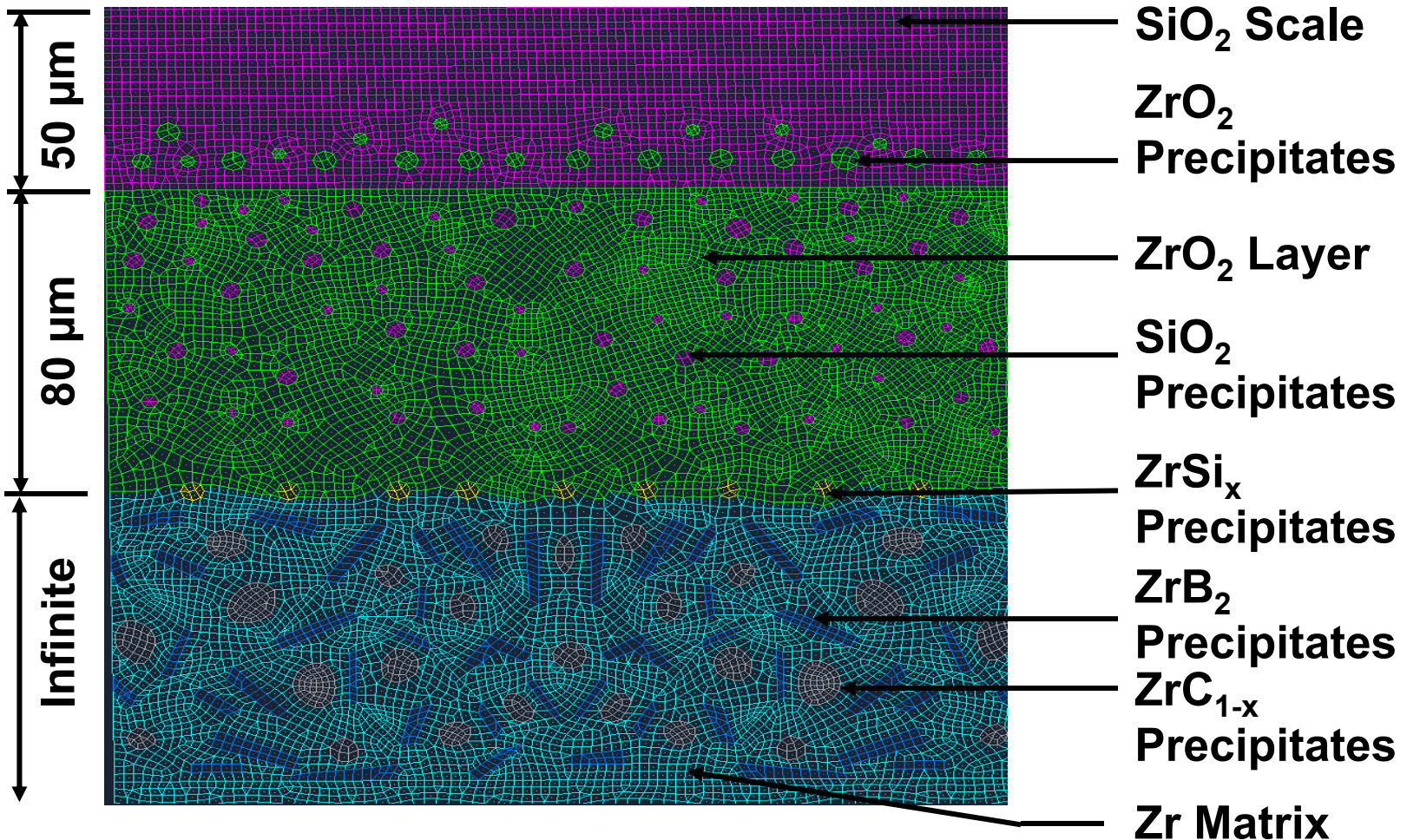
$$u^{XFEM}(x) = \sum_{I \in \mathcal{N}} N_I(x) u_I + \sum_{J \in \hat{\mathcal{N}}} N_J(x) \Psi(x) a_J$$

Standard Part Enriched Part





FEA MODEL OF THE MICROSTRUCTURE OF $ZrB_2 / ZrC_{1-x} / Zr-Si_x$ SYSTEM



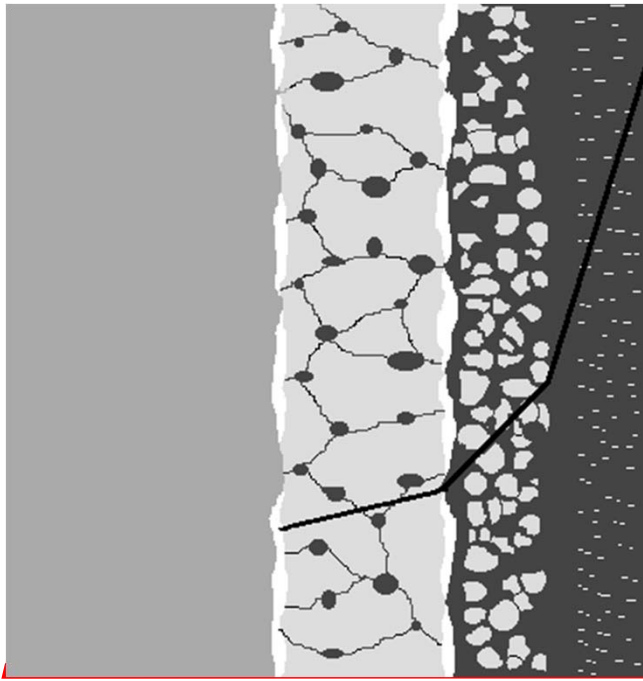
Baseline mesh of the microstructure of ZrB₂ / ZrC_x / Zr-Si SYSTEM

Optimal Configuration of ZrO_2 Precipitates in SiO_2 Matrix

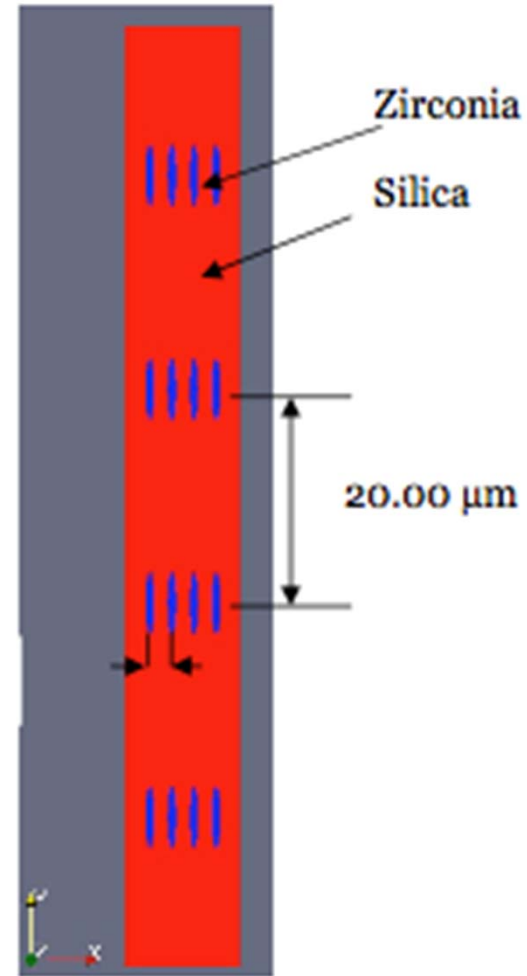
ZrC-ZrB₂-
Zr Matrix

ZrO₂-SiO₂
Layer

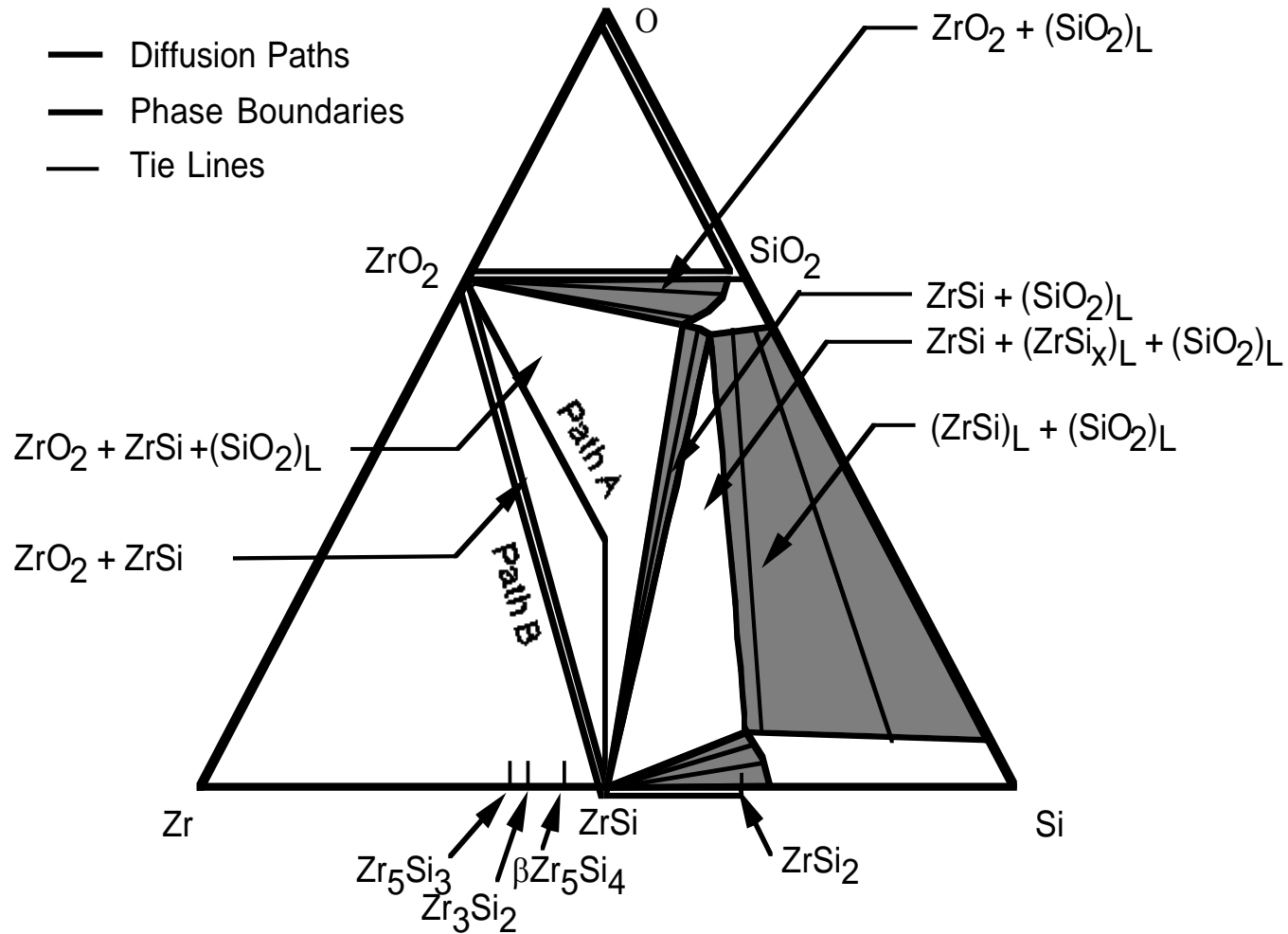
SiO₂-ZrO₂
Scale



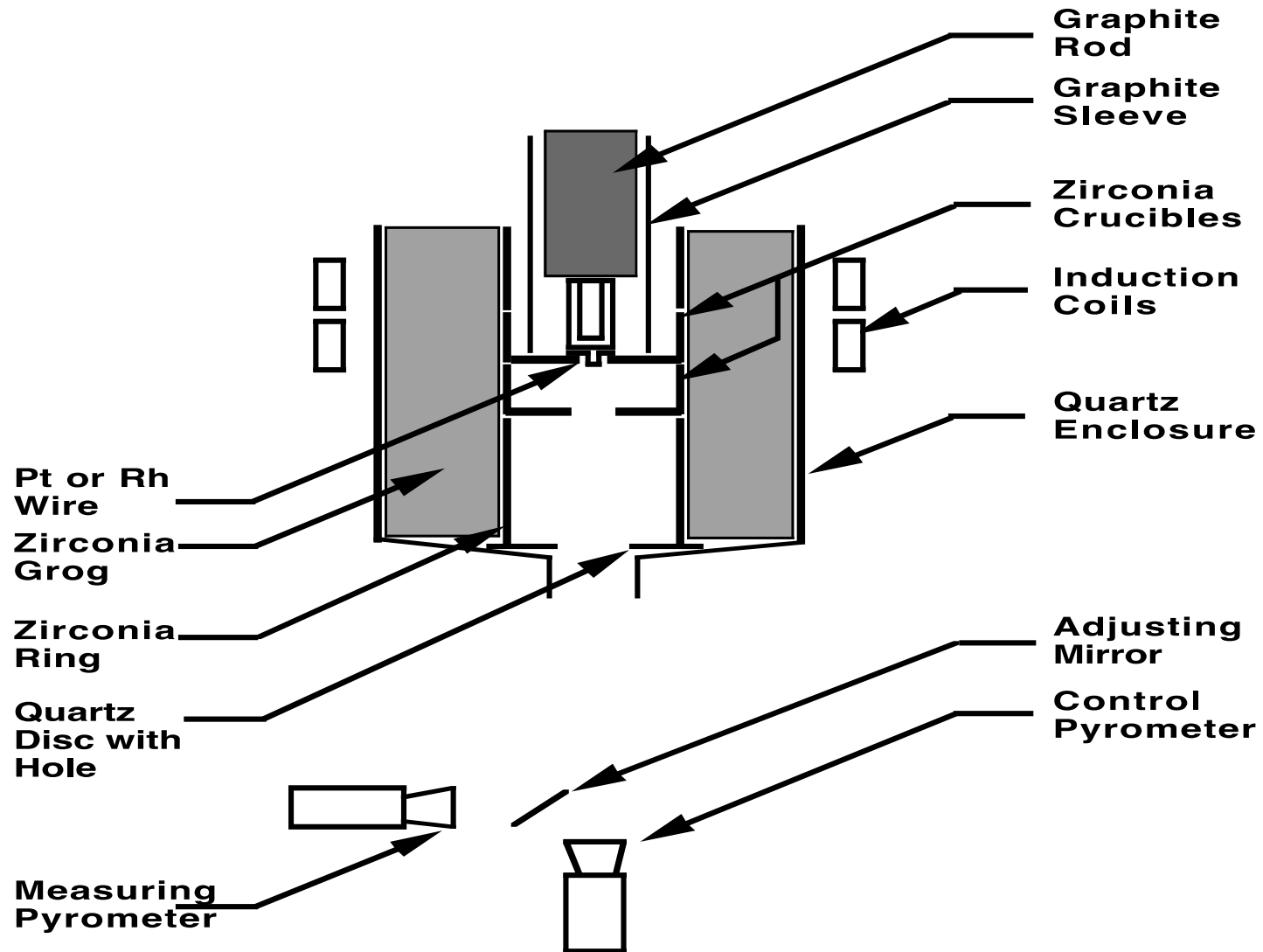
1.96 μm



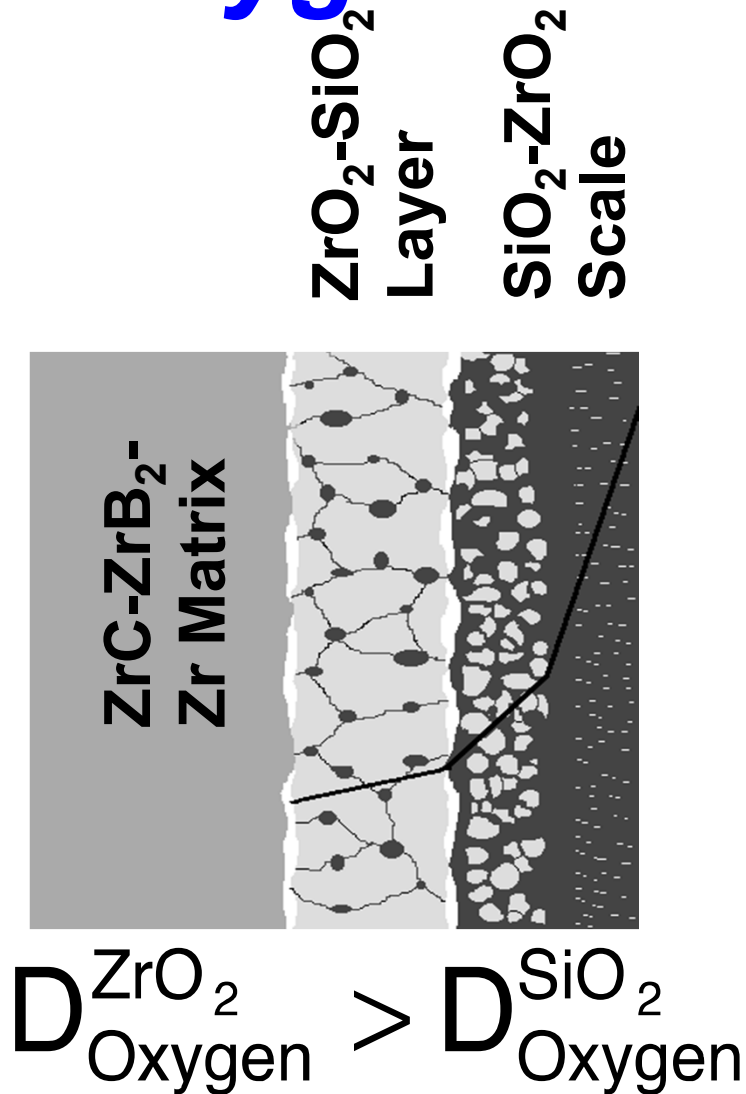
Zr-Si-O Ternary at 1800° C



Furnace Assembly

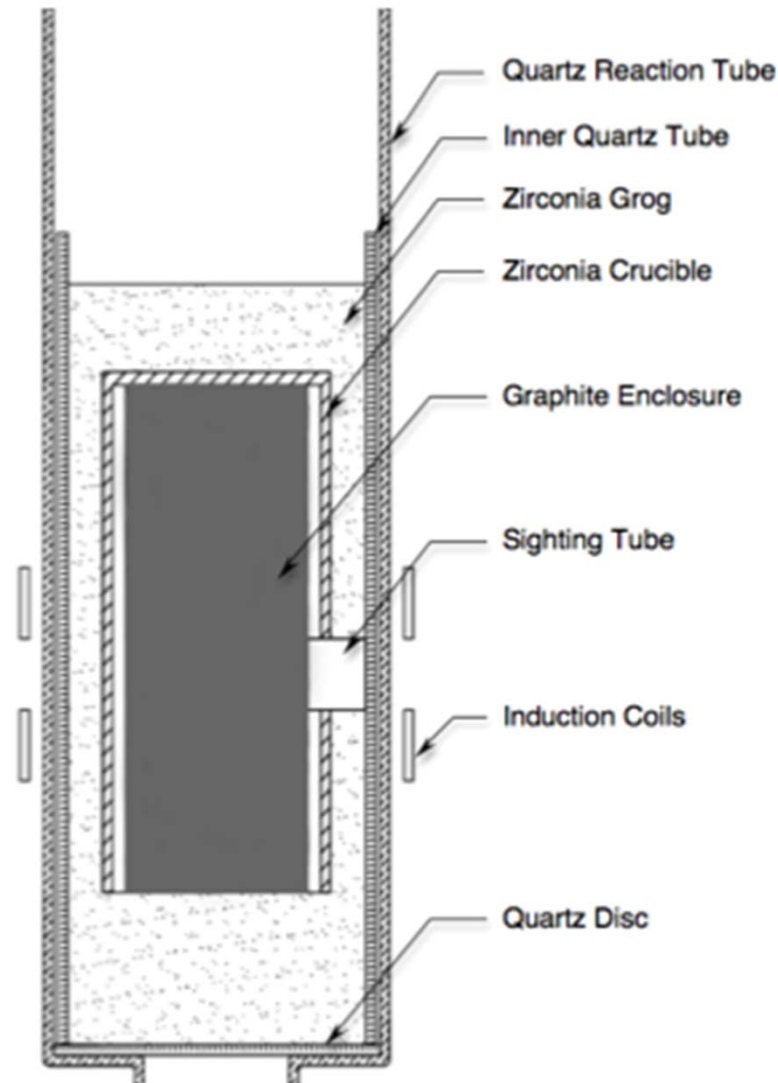


Sketch of Oxygen Diffusion



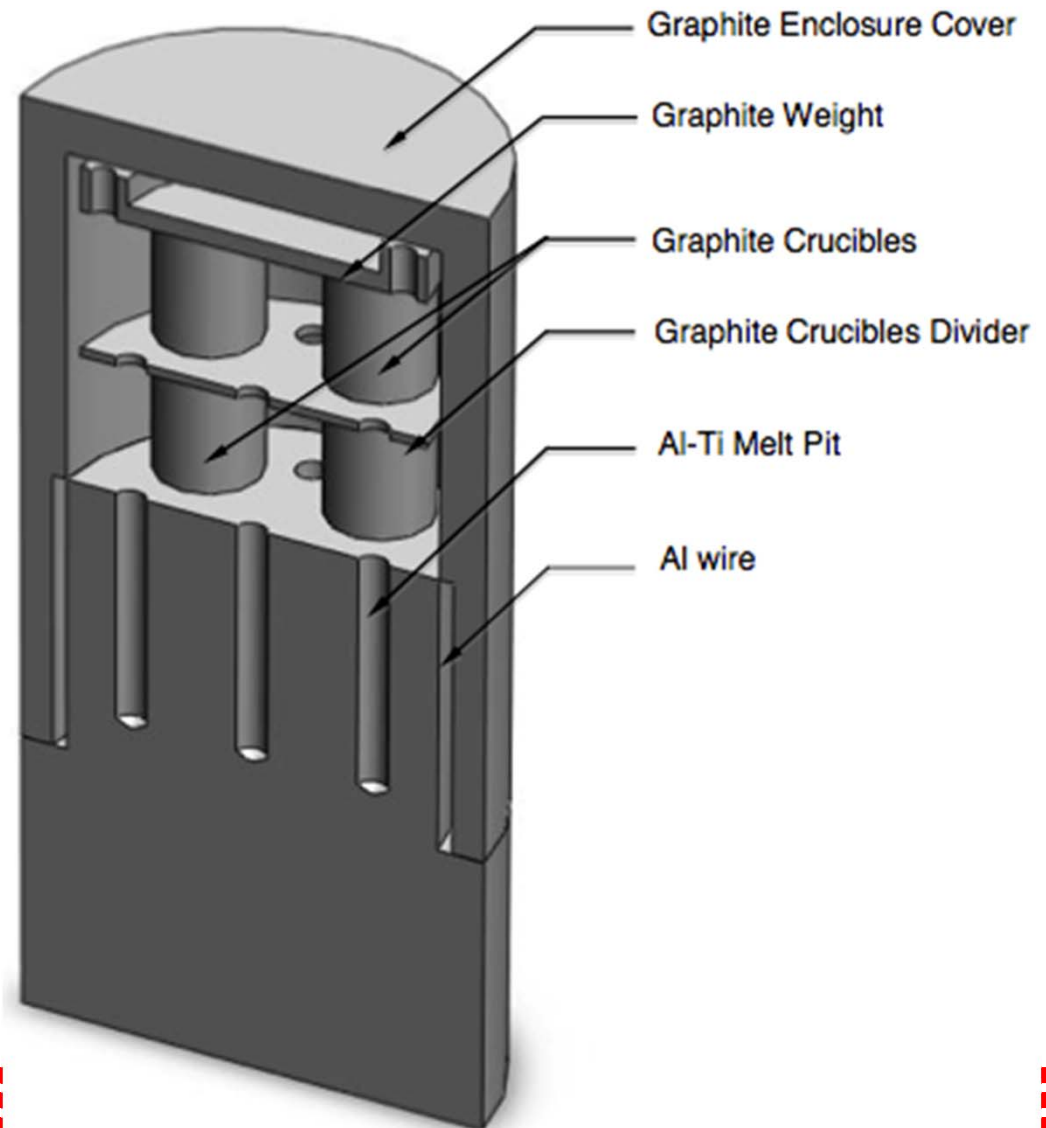
Graphite Enclosure in Dielectric Induction Furnace

- Melted previously ZrO_2 (2983 K)
- Control plasma formation with He and flow rate
- Deoxidized Ar and He flows
- Should improve temperature measurement

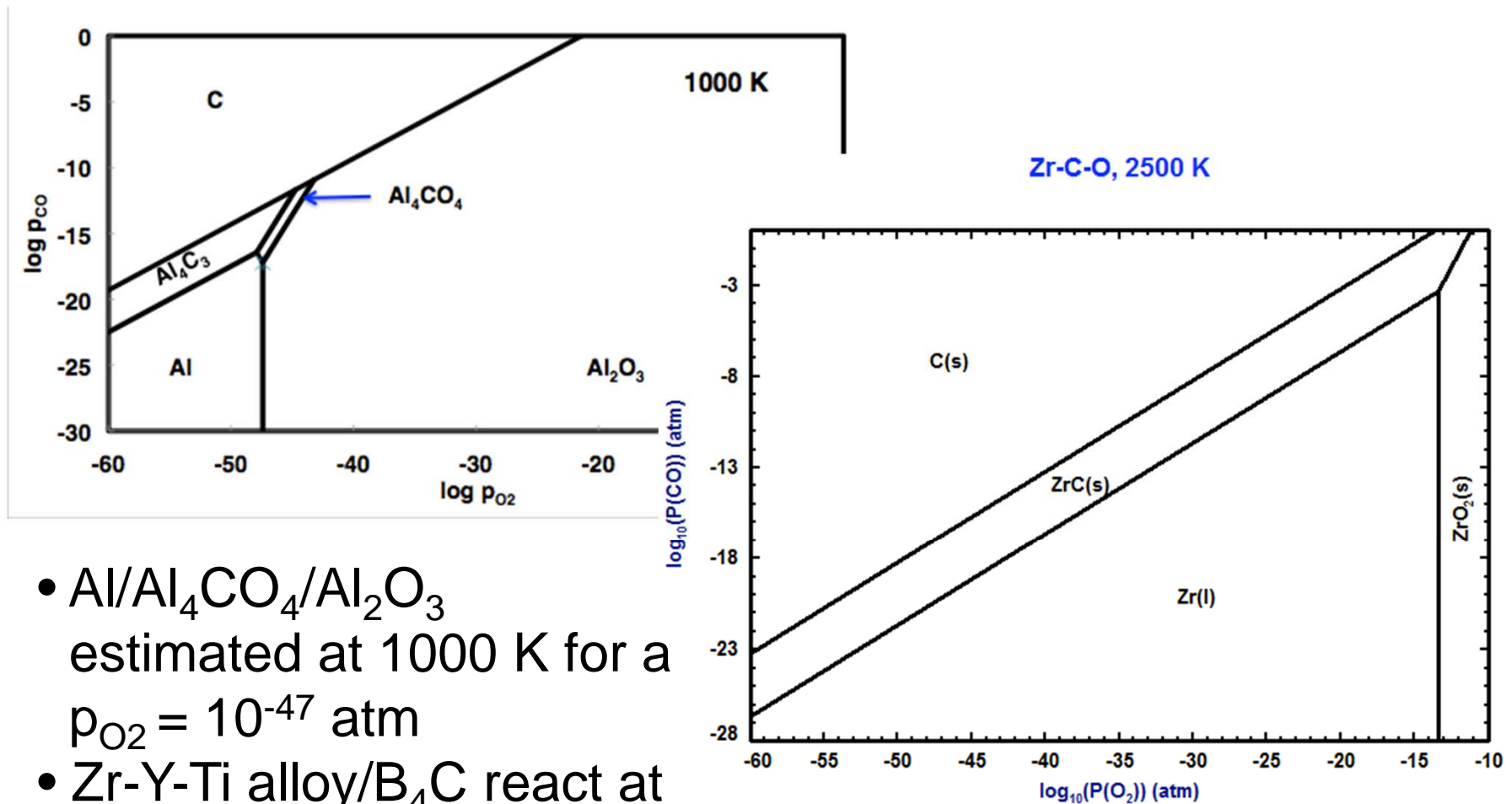


Configuration of Zr alloy/ B_4C reaction system

- Zr-Y-Ti alloy reacting with B_4C contained in graphite crucibles at 2000 K plus.
- Closed thermodynamic system controls oxygen potential.
- Al/ Al_4CO_4 / Al_2O_3 establishes p_{O_2} at 1000 K (follows concept of Komarek research group using pseudo-isopiestic technique).



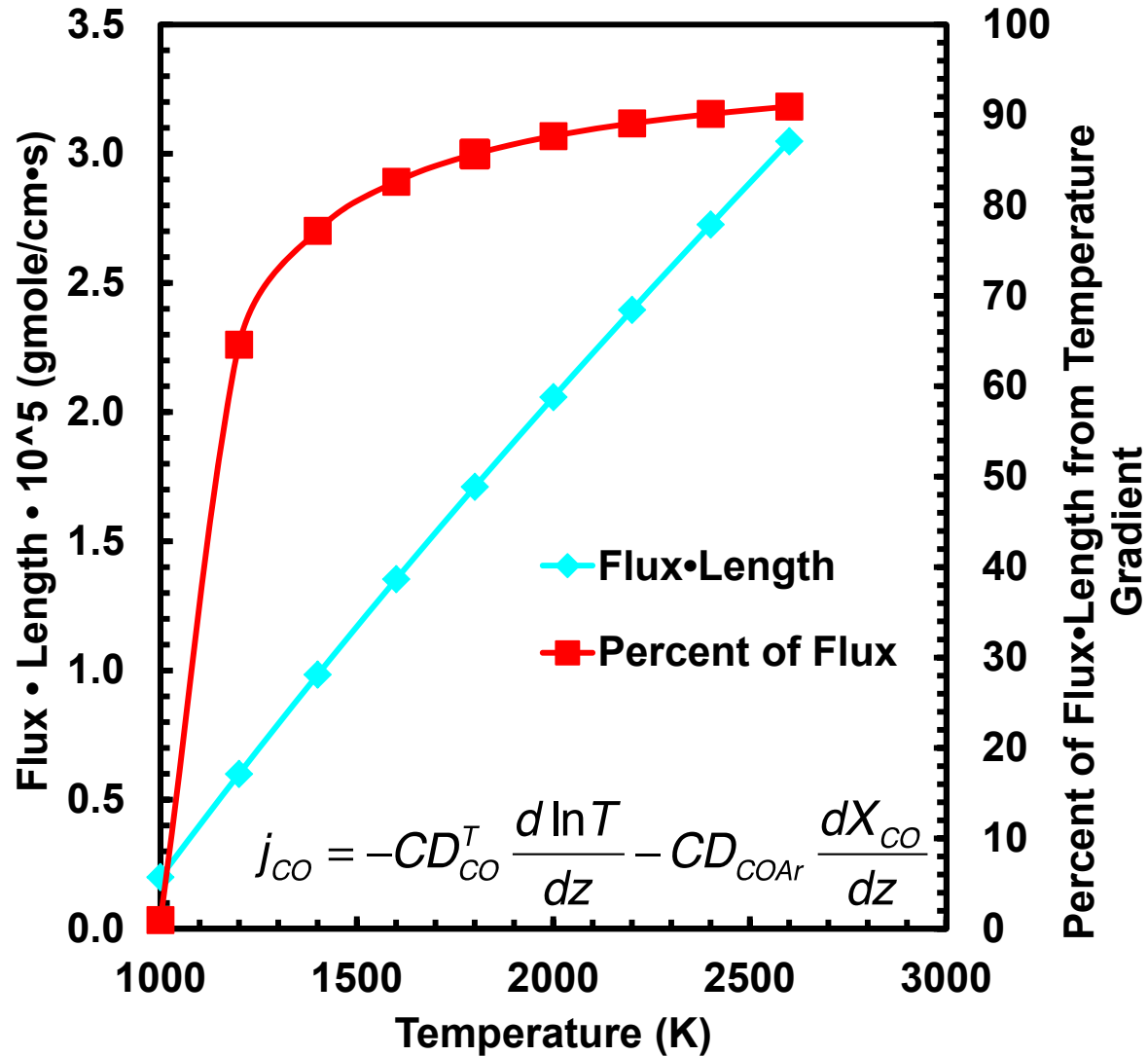
Stability of Al-C-O System at 1000 K and Zr-C-O System at 2500 K



- Al/ Al_4CO_4 / Al_2O_3 estimated at 1000 K for a $p_{O_2} = 10^{-47}$ atm
- Zr-Y-Ti alloy/ B_4C react at > 2125 K



Diffusional Flux – Kinetics Issues

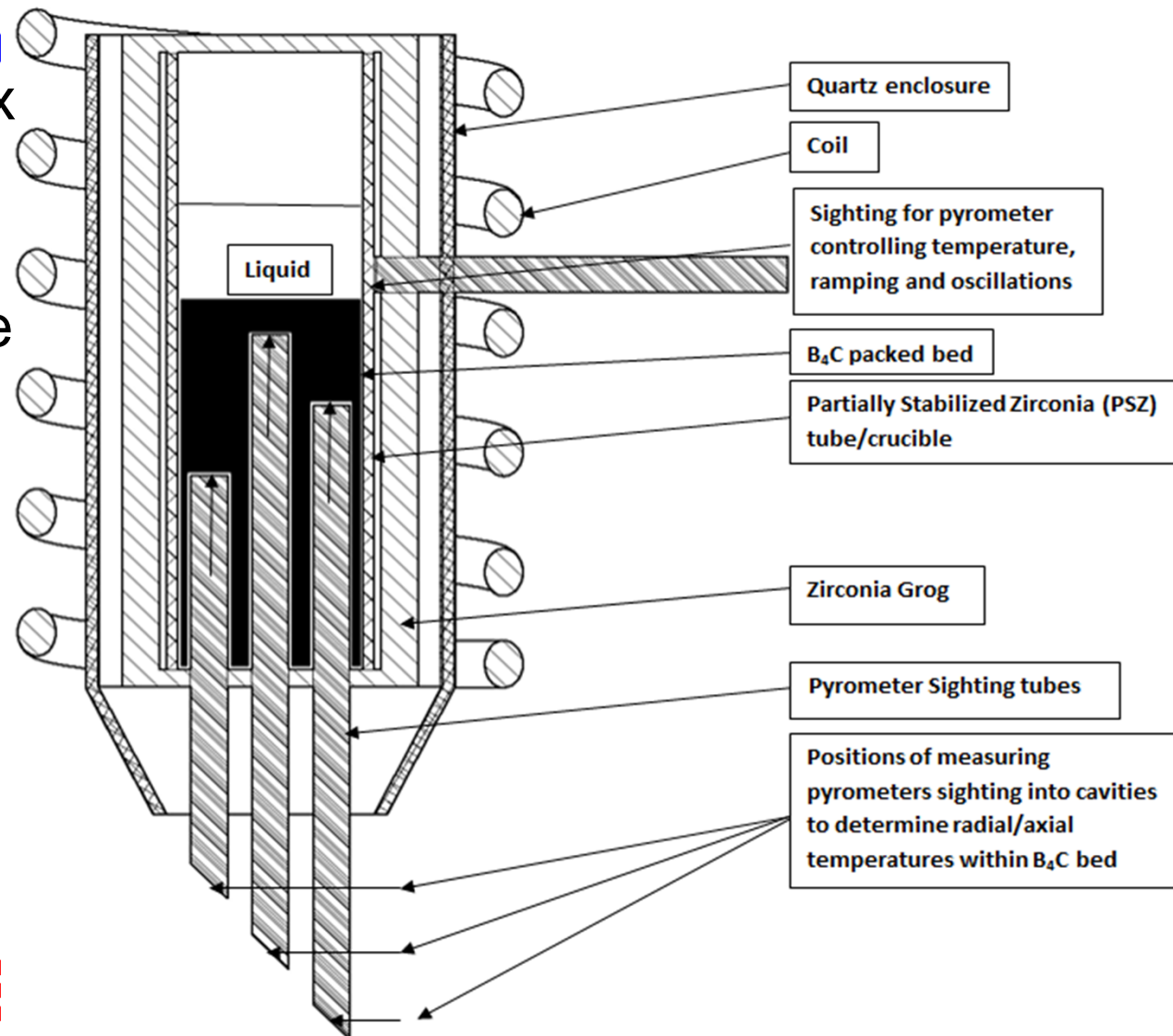


- D_{COAr} from Poirier-Geiger and checked with Chapman-Enskog Eq.
- Mean temperature
$$\frac{T_H T_C}{T_H - T_C} \ln \frac{T_H}{T_C} = 1527K$$
- Al/Al₂O₃/Al₄CO₄ reaction rate?



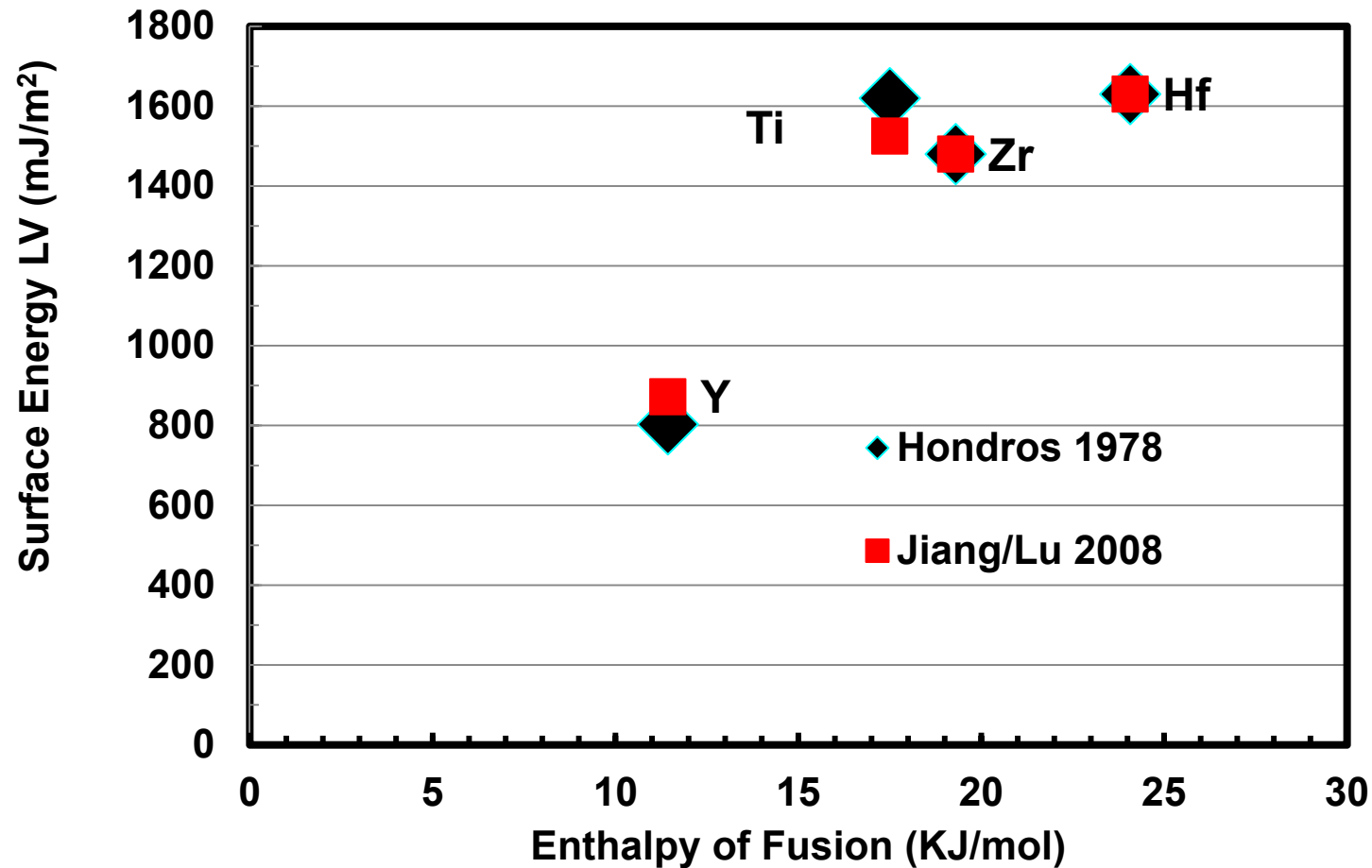
Temperature Measurement of Hf Melt Reacting with B_4C Packed Bed >

- Determine effect of dT/dx on infusion (i.e., σ_{LV})
- Determine the effect of ΔT spike on infusion
- Determine dT/dx on metastable phase formations.



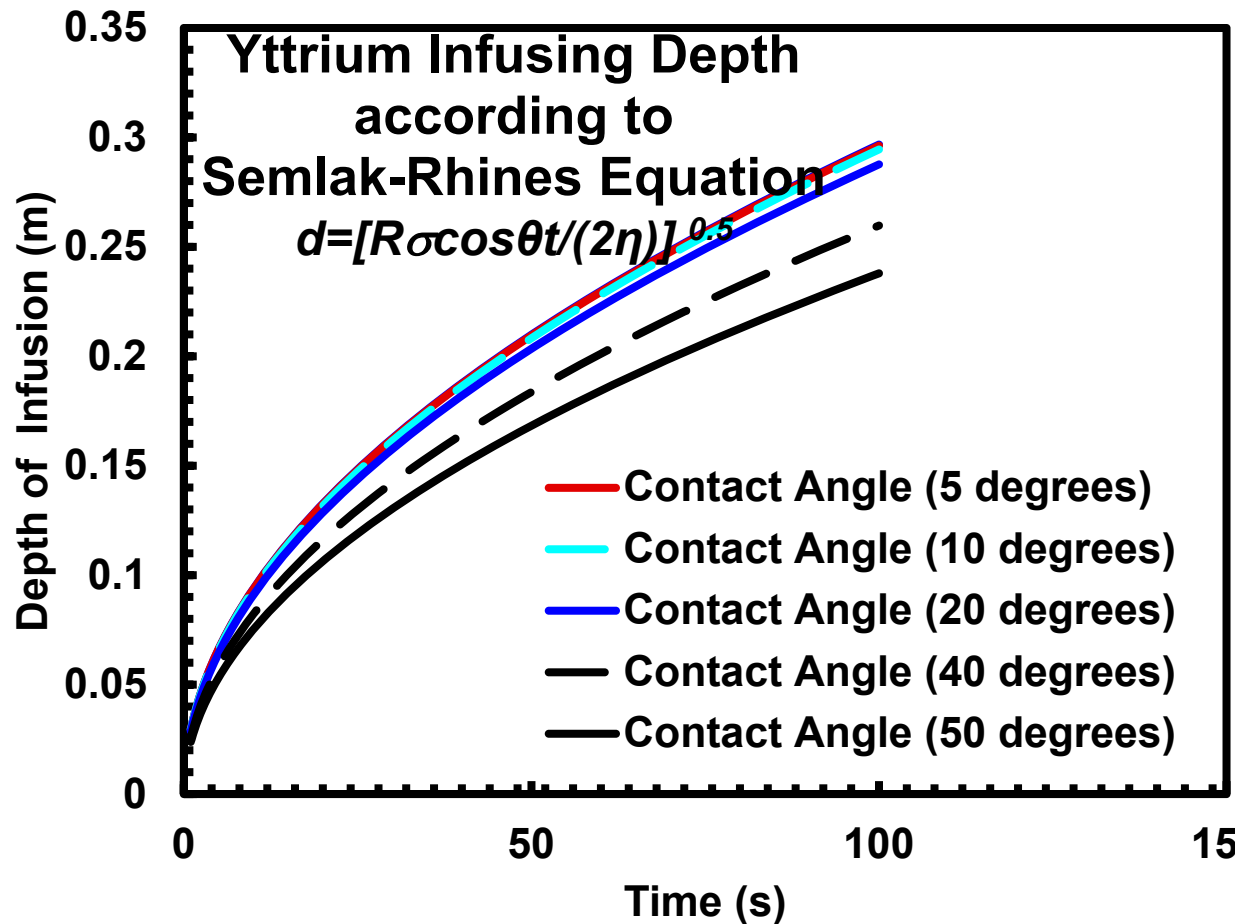


Surface Energies for Hf Alloy Melts Determined from Elements





Depth of Infusion into Packed Bed Driven by Surface Energies



- Expand $d\sigma/dx$ (e.g.,

$$\eta \frac{\partial \mathbf{u}_x}{\partial \mathbf{y}} = \frac{\partial \sigma}{\partial T} \frac{\partial T}{\partial \mathbf{x}}$$

- Use Fluent to model computational fluid dynamics.
- Determine alloying effects (e.g., Hf-Y-Ti)

$$\Gamma_i^{Hf} = -\frac{1}{RT} \left(\frac{\partial \sigma}{\partial \ln p_{O_2}} \right)_{T, i \neq k}$$

- Determine σ with:
 - Butler equation (Yeum, Speiser and Poirier-1989)
 - Multicomponent ΔG incorporating σ using FactSage





Densification of ZrB_2 -TiC- Y_2O_3 (with and without Ta) Composites Using Spark-Plasma Sintering at University of Arizona

Dr. Erica L. Corral¹

Luke S. Walker

Victoria R. Marotto

Dr. Arturo Bronson²

Brenda Mota, Carlos E. Castillo

David Pham, Alvaro Sandate

ZrB_2 -TiC- Y_2O_3 -Ta would react to form ZrO_2 - Y_2O_3 - TiO_2 - Ta_2O_5 determining TiO_2 - Ta_2O_5 glassy phase.

¹ Department of Materials Science and Engineering, Arizona Materials Lab, The University of Arizona, Tucson, AZ

² Mechanical Engineering Department, The University of Texas at El Paso, El Paso, TX





Joint Work Between the Corral Lab and UTEP in Preparing ZrB₂-based ceramics with additions of Ytria and Ta for Improved Oxidation Resistance Through the Formation of Complex Oxide Scales

Material	Composition (wt%)								
	1	2	3	4	5	6	7	8	9
ZrB ₂	79.3	62.0	37.8	33	29	26	30	23	18
TiC	10.3	12.5	15.6	27	36	42	13	19	23
Y ₂ O ₃	10.4	25.5	46.6	40	40	32	37	28	23
Ta*	-	-	-	-	-	-	20	30	36
Temperature (°C)	1600 1650 1700 ^t 1750	1500 1700 1750	1500 1700 1750	1700	1700	1700	1700	1750	1800

Sample volumes of 1.5 cm³ from a 20mm die.

* - Ta foil was finely cut and dispersed in the powder

^t - 3 samples of this composition produced



Compositions for ZrO_2 - Y_2O_3 - TiO_2 - Ta_2O_5 scales

- In t- ZrO_2 /c- ZrO_2 region
- Near c- ZrO_2 /t- ZrO_2 / $TiO_{2,L}$ region
- Near c- ZrO_2 / $Y_2Ti_2O_7$ region
- Ta added for Ta_2O_5 - TiO_2 eutectic scale

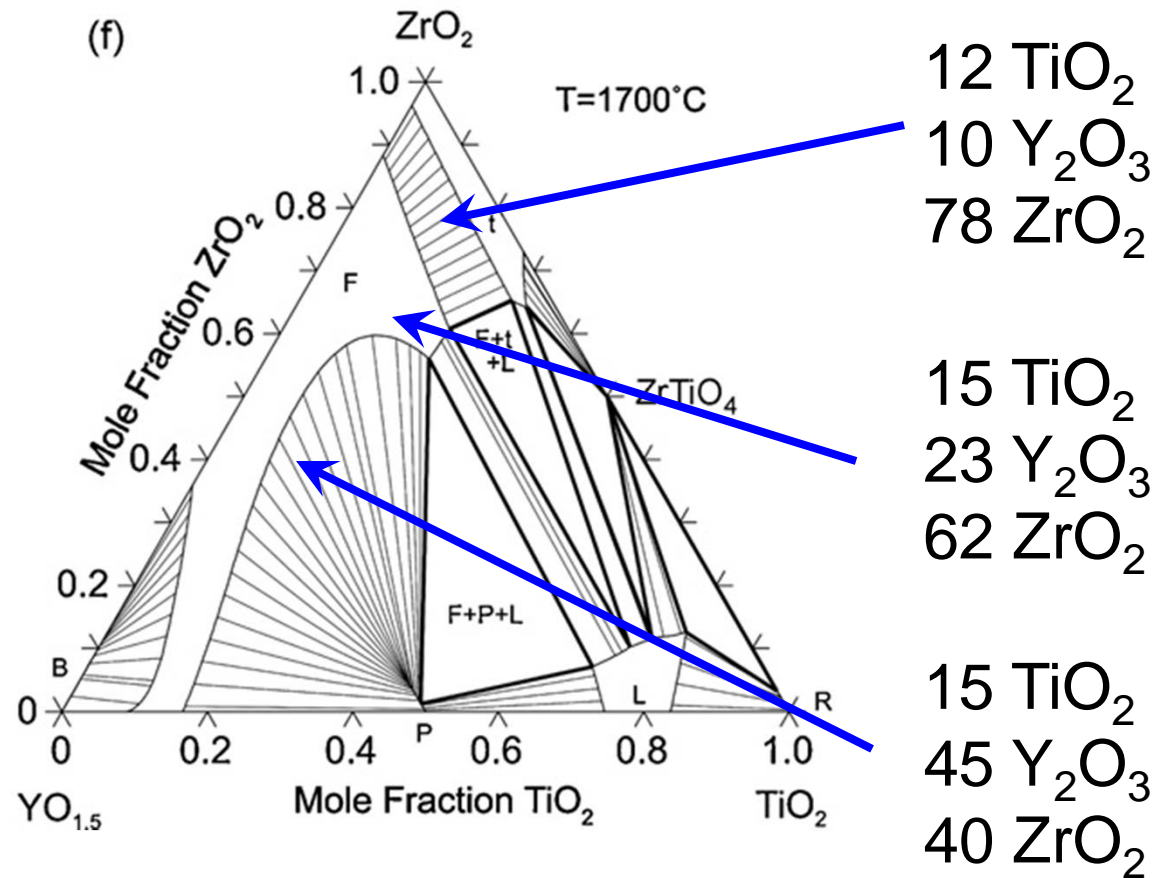


Diagram from Schaedler,
Fabrichnaya and Levi -- 2008